Long-Lived Charge-Separated State Generated in a Ferrocene–*meso,meso*-Linked Porphyrin Trimer–Fullerene Pentad with a High Quantum Yield

Hiroshi Imahori,*[a] Yuji Sekiguchi,[b] Yukiyasu Kashiwagi,[b] Tohru Sato,[a] Yasuyuki Araki,[c] Osamu Ito,*[c] Hiroko Yamada,[b] and Shunichi Fukuzumi*[b]

Abstract: A *meso,meso*-linked porphyrin trimer, $(ZnP)_3$, as a light-harvesting chromophore, has been incorporated for the first time into a photosynthetic multistep electron-transfer model including ferrocene (Fc) as an electron donor and fullerene (C_{60}) as an electron acceptor, to construct the ferrocene–*meso,meso*-linked porphyrin trimer–fullerene system **Fc-(ZnP)$_3$-C$_{60}$**. Photoirradiation of **Fc-(ZnP)$_3$-C$_{60}$** results in photoinduced electron transfer from both the singlet and triplet excited states of the porphyrin trimer, $^1(ZnP)_3^*$ and $^3(ZnP)_3^*$, to the C_{60} moiety to produce the porphyrin trimer radical cation–C_{60} radical anion pair, **Fc-(ZnP)$_3$$^{\cdot+}$-C$_{60}$$^{\cdot-}$**. Subsequent formation of the final charge-separated state **Fc$^+$-(ZnP)$_3$-C$_{60}$$^{\cdot-}$** was confirmed by the transient absorption spectra observed by pico- and nanosecond time-resolved laser flash photolysis. The final charge-separated state decays, obeying first-order kinetics, with a long lifetime (0.53 s in DMF at 163 K) that is comparable with that of the natural bacterial photosynthetic reaction center. More importantly, the quantum yield of formation of the final charge-separated state (0.83 in benzonitrile) remains high, despite the large separation distance between the Fc^+ and $C_{60}^{\cdot-}$ moieties. Such a high quantum yield results from efficient charge separation through the porphyrin trimer, whereas a slow charge recombination is associated with the localized porphyrin radical cation in the porphyrin trimer. The light-harvesting efficiency in the visible region has also been much improved in **Fc-(ZnP)$_3$-C$_{60}$** because of exciton coupling in the porphyrin trimer as well as an increase in the number of porphyrins.

Keywords: donor–acceptor systems · electron transfer · fullerenes · photosynthesis · porphyrinoids

Introduction

The three-dimensional structures of the antenna complex and the bacterial reaction center have provided an important structural basis for understanding the light-harvesting and subsequent primary charge separation processes in photosynthesis:[1,2] visible light is harvested by the antenna complexes, including a wheel-like array of chlorophylls and carotenoid polyenes, and the collected energy is funneled efficiently into the chlorophyll dimer (that is, special pair) in the reaction center. The subsequent multistep electron-transfer (ET) event takes place unidirectionally along the well-arranged chromophores that are embedded in the transmembrane protein in the sequence special pair, accessory chlorophyll, pheophytin, quinones. The charge-separated state lasts for seconds in nearly 100% quantum yield, and leads eventually to the conversion of light into usable chemical energy. The importance and complexity of energy transfer (EN) and ET reactions in photosynthesis have inspired many chemists to design and prepare donor–acceptor linked systems that mimic the EN or ET processes.[3–11]

Since chlorophylls are essential components in the photosynthetic reaction center, porphyrins and metalloporphyrins have frequently been employed as their analogues in donor–acceptor-linked molecules.[3–10] Some of the covalently linked porphyrin-containing arrays, such as triads, tetrads, and pentads, have successfully exhibited efficient EN or ET

[a] Prof. Dr. H. Imahori, Dr. T. Sato
Department of Molecular Engineering, Graduate School of Engineering, Kyoto University
PRESTO, Japan Science and Technology Corporation (JST)
Katsura, Nishikyo-ku, Kyoto 615–8510 (Japan)
and
Fukui Institute for Fundamental Chemistry, Kyoto University
34–4, Takano-Nishihiraki-cho, Sakyo-ku, Kyoto 606–8103 (Japan)
E-mail: imahori@scl.kyoto-u.ac.jp

[b] Y. Sekiguchi, Y. Kashiwagi, Dr. H. Yamada, Prof. Dr. S. Fukuzumi
Department of Material and Life Science, Graduate School of Engineering, Osaka University
CREST, Japan Science and Technology Corporation (JST), Suita
Osaka 565–0871 (Japan)
E-mail: fukuzumi@ap.chem.eng.osaka-u.ac.jp

[c] Dr. Y. Araki, Prof. Dr. O. Ito
Institute of Multidisciplinary Research for Advanced Materials
Tohoku University
CREST, JST, Katahira, Aoba-ku, Sendai 980–8577 (Japan)
E-mail: ito@tagen.tohoku.ac.jp

DOI: 10.1002/chem.200305308

processes such as photosynthesis. However, the difficulty of synthesis has precluded integration of the two functions, light harvesting and charge separation, into one artificial system. So far there have been few examples of donor–acceptor-linked systems mimicking both EN and ET processes in photosynthesis.[12]

Recently we synthesized the longest-lived charge-separated state in the ferrocene–zinc porphyrin–free-base porphyrin–fullerene tetrad **Fc-ZnP-H_2P-C_{60}** (Scheme 1), which reveals a cascade of photoinduced energy transfer and multistep electron transfer within a molecule in frozen media as well as in solution.[13] The lifetime of the resulting charge-separated state (ferricenium ion–C_{60} radical anion pair) in frozen benzonitrile (PhCN) is as long as 0.38 s, which is comparable with that observed for the bacterial photosynthetic reaction center. However, the quantum yield for formation of the charge-separated state ($\Phi = 0.24$) is still much lower than that of the natural system ($\Phi = 1$). Thus, the charge separation efficiency could still be much improved. Moreover, the light-harvesting efficiency could also be increased. In this context, *meso,meso*-porphyrin arrays are good candidates to improve both efficiencies, since their length can be extended easily by facile oligomerization of the porphyrin monomer.[14–17] In addition, they can absorb visible light over a wider spectrum than a linear combination of the corresponding porphyrin monomers, because of the exciton coupling of the porphyrins, as in molecular assemblies of chlorophylls in antenna complexes.[1,2] We have previously reported incorporation of the *meso,meso*-linked porphyrin dimer $(ZnP)_2$, as an improved light-harvesting chromophore compared with the monomer porphyrin, into a photosynthetic ET model to construct the ferrocene–*meso*,-

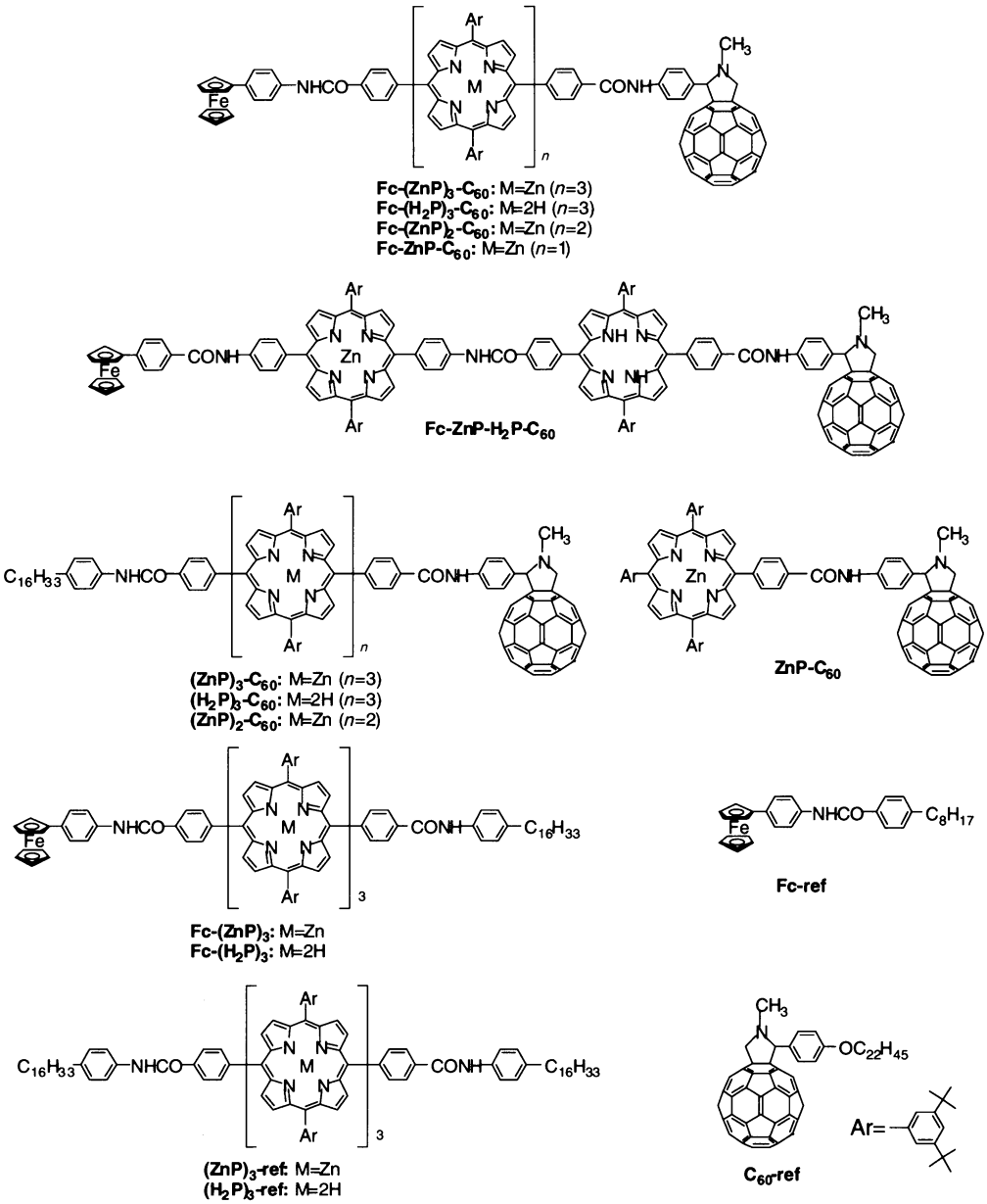

Scheme 1. Ferrocene–porphyrin trimer–fullerene pentad and the reference compounds.

meso-linked porphyrin dimer–fullerene tetrad **Fc-(ZnP)$_2$-C$_{60}$** (Scheme 1), in which the C_{60} and the ferrocene (Fc) are tethered at both ends of $(ZnP)_2$.[18] The quantum yield of formation of the final charge-separated state (0.80 in PhCN) is indeed improved. However, this final state decays obeying first-order kinetics with a lifetime of 19 μs in PhCN at 295 K, which is far shorter than the value expected from the long edge-to-edge distance (R_{ee} = 38.6 Å) as compared with the R_{ee} value of **Fc$^+$-ZnP-C$_{60}$$^{\cdot-}$** radical ion pair ($R_{ee}$ = 30.3 Å), which has a lifetime of up to 16 μs in PhCN.[19]

We report herein incorporation of an additional porphyrin moiety to construct the ferrocene–*meso*,*meso*-linked porphyrin trimer–fullerene pentad **Fc-(ZnP)$_3$-C$_{60}$**, in which the C_{60} and the ferrocene (Fc) are tethered at both the ends of $(ZnP)_3$ (R_{ee} = 46.9 Å) (Scheme 1). The lifetime of the final charge-separated state is expected to be prolonged without lowering the charge separation (CS) efficiency, provided that a similar stepwise ET occurs in **Fc-(ZnP)$_3$-C$_{60}$**. We have achieved not only a high quantum yield for the formation of a final charge-separated state (Φ = 0.83), but also a longer lifetime of the charge-separated state than the previously reported longest lifetime of **Fc-ZnP-H$_2$P-C$_{60}$**.[13] The light-harvesting efficiency has also been much improved in **Fc-(ZnP)$_3$-C$_{60}$** as compared with **Fc-ZnP-H$_2$P-C$_{60}$**,[13] **Fc-ZnP-C$_{60}$**[19] and **Fc-(ZnP)$_2$-C$_{60}$**.[18] The ET dynamics of **Fc-(ZnP)$_3$-C$_{60}$** has been investigated by ESR spectroscopy as well as by time-resolved transient absorption spectroscopy and fluorescence lifetime measurements.

Results and Discussion

Synthesis: **Fc-(ZnP)$_3$-C$_{60}$**, the reference tetrads **Fc-(ZnP)$_3$** and **(ZnP)$_3$-C$_{60}$**, and the porphyrin reference **(ZnP)$_3$-ref** (Scheme 1) were prepared as shown in Scheme 2. For the *meso*,*meso* coupling of **1**[18,20,21] and **2**,[14] we used the oxidant $AgPF_6$ in a mixture of chloroform and acetonitrile. Because slight demetallation occurred under the present experimental conditions, the crude mixture was treated with TFA and H_2SO_4 in chloroform to afford free-base porphyrin **3**. The resulting coupling reaction mixture contained the other porphyrin derivatives, such as homo- and hetero-coupled mono-, di-, tri-, and tetra-*meso*,*meso*-porphyrins. The free-base porphyrin **3** was purified by silica gel column chromatogra-

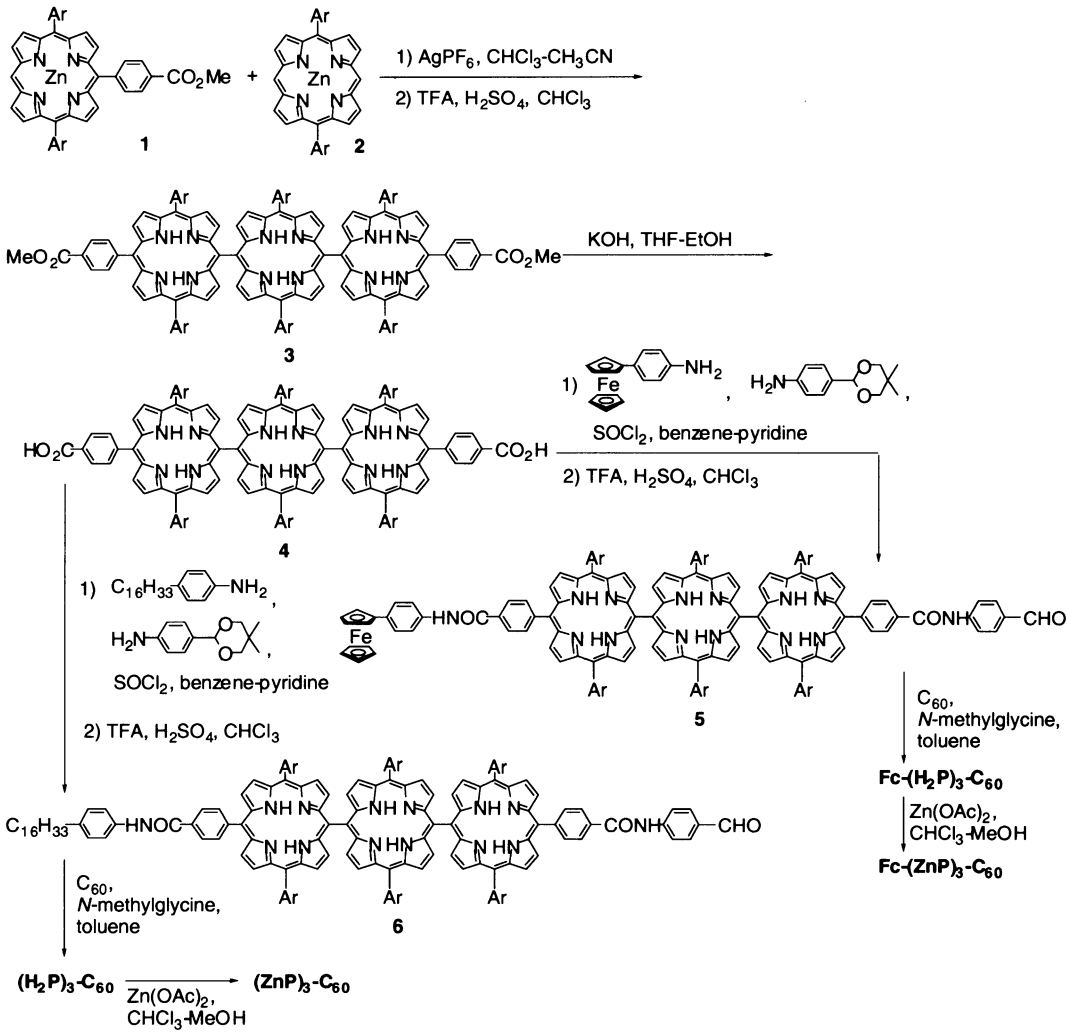

Scheme 2. Synthesis of ferrocene–porphyrin trimer–fullerene pentad and the reference compounds.

phy and gel permeation chromatography. Important synthetic intermediate **4** was obtained by base hydrolysis of **3** in a mixture of THF and ethanol. The free-base porphyrin carboxylic acid **4** was converted to the corresponding bis(acid chloride) by treatment with $SOCl_2$ (Scheme 2). Cross-condensation with 4-aminophenylferrocene[19] and formyl-protected aniline[22] in benzene in the presence of pyridine, followed by acid hydrolysis, afforded ferrocene–*meso*,*meso*-linked porphyrin trimer **5** in 19% yield.

Fc-(ZnP)$_3$-C$_{60}$ was obtained in 65% yield by 1,3-dipolar cycloaddition[23] using **5**, *N*-methylglycine, and C_{60} in toluene and subsequent treatment with zinc acetate.

(ZnP)$_3$-C$_{60}$ was synthesized from 4-hexadecylaniline, **4**, and formyl-protected aniline via **6** by the method described for **Fc-(ZnP)$_3$-C$_{60}$**. **Fc-(ZnP)$_3$** and **(ZnP)$_3$-ref** were prepared from 4-aminophenylferrocene, **4**, and 4-hexadecylaniline, and **4** and 4-hexadecylaniline, respectively. Single-chromophore references **Fc-ref**[19] and **C$_{60}$-ref**[13] were also prepared by following the same procedures as described previously. Their structures were verified by spectroscopic analyses including ^{1}H NMR, FAB, and MALDI-TOF mass spectra (see Experimental Section).

Absorption and fluorescence spectra: The absorption spectrum of **Fc-(ZnP)$_3$-C$_{60}$** in PhCN is virtually a linear combination of the spectra of **Fc-ref**, **(ZnP)$_3$-ref**, and **C$_{60}$-ref**. This indicates that there is no significant interaction among the three chromophores in the ground state. The absorption of the porphyrin trimer in the visible region is much stronger than that of the ferrocene and the C_{60} moieties. It should be noted that the splitting of the Soret bands ($\approx$430 nm and $\approx$ 490 nm) is characteristic of the *meso*,*meso*-linked porphyrins,[14],[15] as in Figure 1. This enables us to harvest the light more widely across the visible region than does a linear combination of zinc porphyrin monomer **1** or **2**. **Fc-(ZnP)$_3$-C$_{60}$** absorbs visible light more widely than **Fc-ZnP-C$_{60}$** or **Fc-(ZnP)$_2$-C$_{60}$** (Figure 1).

The steady-state fluorescence spectrum of **Fc-(ZnP)$_3$-C$_{60}$** in PhCN exhibits the same band shape and peak positions as **(ZnP)$_3$-ref** (λ_{em}^{max} = 651 nm). No emission from the C_{60} (λ_{em}^{max} = 720 nm)[24] could be detected for **Fc-(ZnP)$_3$-C$_{60}$**. The fluorescence spectrum of **Fc-(ZnP)$_3$-C$_{60}$** in PhCN is strongly quenched compared with that of **(ZnP)$_3$-ref** (relative intensity for **Fc-(ZnP)$_3$-C$_{60}$** = 0.13) when adjusting absorbance (0.32) at the excitation wavelength of 426 nm, where the porphyrin moiety absorbs light exclusively. In contrast, the fluorescence spectrum of **Fc-(ZnP)$_3$** in PhCN is more weakly quenched than that of **(ZnP)$_3$-ref** (relative intensity for **Fc-(ZnP)$_3$** = 0.83). This indicates that an electron transfer occurs mainly from the singlet excited state $^1(ZnP)_3^*$ to C_{60} rather than from Fc to $^1(ZnP)_3^*$ (vide infra).

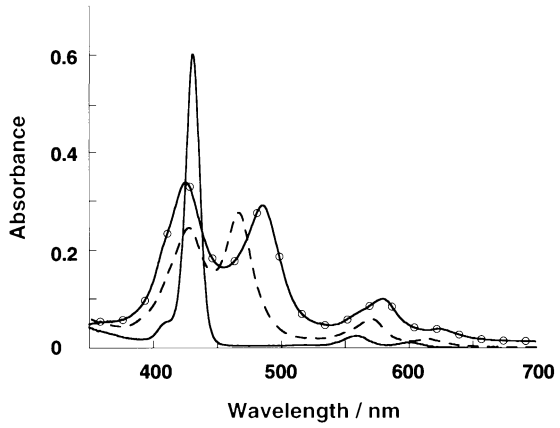

Figure 1. Absorption spectra of **Fc-(ZnP)$_3$-C$_{60}$** (solid line with open rings), **Fc-(ZnP)$_2$-C$_{60}$** (broken line), and **Fc-ZnP-C$_{60}$** (solid line) in PhCN (1.0×10^{-6} M).

One-electron redox potentials and ET driving force: The driving forces ($-\Delta G^{o}_{ET}$) for all the intramolecular ET processes were determined accurately by measuring the redox potentials of reference chromophores (**Fc-ref**, **(ZnP)$_3$-ref**, and **C$_{60}$-ref**) in PhCN, THF, and DMF. The differential pulse voltammetry was performed in PhCN, THF, and DMF containing nBu$_4$NPF$_6$ (0.1 M) as a supporting electrolyte. Table 1 summarizes all the redox potentials of the compounds investigated, and of **Fc-ref** and **C$_{60}$-ref** as references, which were reported previously.[13] The first one-electron oxidation potentials (E^{o}_{ox}) of **(ZnP)$_3$-ref** and **Fc-ref** are 0.32 V and $-$0.01 V versus ferrocene/ferricenium (Fc/Fc$^+$) and the first one-electron reduction potentials (E^{0}_{red}) of **C$_{60}$-ref** and **(ZnP)$_3$-ref** are $-$1.04 V and $-$1.83 V versus Fc/Fc$^+$ in PhCN, respectively.

Table 1. One-electron redox potentials (versus Fc/Fc$^+$)[a] of references in PhCN, THF, and DMF.

Compound	Solvent	E^0_{ox} [V] $(ZnP)_3^{\cdot+}$/$(ZnP)_3$	E^0_{ox} [V] Fc$^+$/Fc	E^0_{red} [V] $C_{60}/C_{60}^{\cdot-}$	E^0_{red} [V] $(ZnP)_3$/$(ZnP)_3^{\cdot-}$
(ZnP)$_3$-ref	PhCN	0.32			$-$1.83
Fc-ref			$-$0.01[b]		
C$_{60}$-ref				$-$1.04[b]	
(ZnP)$_3$-ref	THF	0.33			$-$1.96
Fc-ref			$-$0.02[b]		
C$_{60}$-ref				$-$1.02[b]	
(ZnP)$_3$-ref	DMF	0.33			$-$1.94[b]
Fc-ref			$-$0.01[b]		
C$_{60}$-ref				$-$0.92[b]	

[a] The redox potentials were measured by differential pulse voltammetry in PhCN using 0.1 M nBu$_4$NPF$_6$ as a supporting electrolyte with a sweep rate of 10 mV s^{-1}. [b] From ref. [13].

The driving forces ($-\Delta G^{0}_{ET(CR)}$ [eV]) for the intramolecular CR processes from the C_{60} radical anion ($C_{60}^{\cdot-}$) to the zinc porphyrin trimer radical cation [$(ZnP)_3^{\cdot+}$] or the ferricenium ion (Fc$^+$) in **Fc-(ZnP)$_3$-C$_{60}$** and **(ZnP)$_3$-C$_{60}$** were determined by applying Equation (1), where e stands for the elementary charge. The $-\Delta G^{0}_{ET(CR)}$ values [eV] in PhCN, THF, and DMF thus obtained are listed in Tables 2 and 3.

$$-\Delta G^{0}_{ET(CR)} = e[E^{0}_{ox}(D^{\cdot+}/D) - E^{0}_{red}(A/A^{\cdot-})] \quad (1)$$

The driving forces for the intramolecular charge separation processes ($-\Delta G^{0}_{ET(CS)}$ [eV]) from the porphyrin trimer singlet and triplet excited states to the C_{60} moiety in **Fc-**

(ZnP)$_3$-C$_{60}$ and **(ZnP)$_3$-C$_{60}$** were determined by Equation (2), where ΔE_{0-0} is the energy of the 0–0 transition energy gap between the lowest singlet or triplet excited state and the ground state, which is determined by the 0–0* absorption and 0*–0 fluorescence or phosphorescence maxima in a solvent (* denotes the excited state). The $-\Delta G^0_{ET(CS)}$ values are given in Table 2 and 3. The driving forces for intramolecular charge-shift (CSH) processes ($-\Delta G^0_{ET(CSH)}$ [eV]) from the Fc to the $(ZnP)_3^{\bullet+}$ moiety in **Fc-(ZnP)$_3$-C$_{60}$** were determined by subtracting the energy of the final state from that of the initial state (Table 3). The Coulombic terms in the present donor–acceptor systems are largely neglected in the evaluation of the driving forces in Tables 2 and 3, especially in solvents with moderate or high polarity, because of the relatively long edge-to-edge distance ($R_{ee} > 11$ Å) employed.

$$-\Delta G^0_{ET(CS)} = \Delta E_{0-0} + \Delta G^0_{ET(CR)} \quad (2)$$

Photodynamics of porphyrin–fullerene-linked systems: Time-resolved transient absorption spectra, following pico- and nanosecond laser pulses, were employed to examine the photodynamics of **(ZnP)$_3$-ref**, **(ZnP)$_3$-C$_{60}$**, **Fc-(ZnP)$_3$**, and **Fc-(ZnP)$_3$-C$_{60}$**. To monitor the intramolecular ET dynamics, the absorption of the one-electron reduced form of the electron acceptor ($C_{60}^{\bullet-}$) was analyzed in the near-IR region around 1000 nm.

(ZnP)$_3$-ref: Picosecond excitation (560 nm) of **(ZnP)$_3$-ref** resulted in characteristic absorption changes in 500–700 nm range (Figure 2, dotted line). In particular, a net decrease of the absorption was observed around 580 nm, which is dominated by the strong ground-state absorption. This suggests that the porphyrin singlet ground state is converted to the corresponding singlet excited state $^1(ZnP)_3^*$.[25] $^1(ZnP)_3^*$ also exhibits a strong absorption band at 520 nm. Intersystem crossing is the predominant fate of the singlet excited state. The resultant triplet excited state $^3(ZnP)_3^*$[25] reveals a characteristic peak in the nanosecond absorption spectrum around 820 nm (Figure 3a), whereas no characteristic absorption around 800–1050 nm appears in the picosecond spectrum (Figure 2). The lifetimes determined for the porphyrin trimer triplet excited state are 1.1 ms in PhCN, 1.7 ms in THF, and 1.1 ms in DMF.

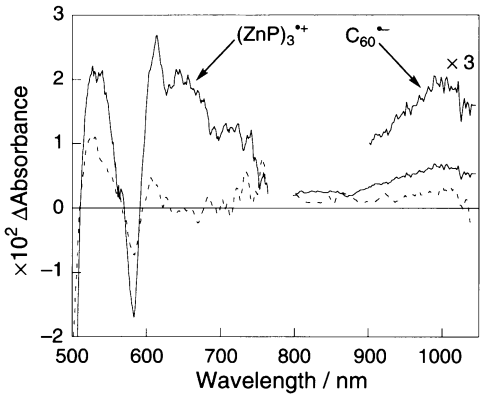

Figure 2. Picosecond time-resolved absorption spectra of **(ZnP)$_3$-ref** (dotted line) and **(ZnP)$_3$-C$_{60}$** (solid line) at a time delay of 1000 ps excited at 560 nm in argon-saturated PhCN.

The porphyrin trimer radical cation $(ZnP)_3^{\bullet+}$ produced by the chemical oxidation of **(ZnP)$_3$-ref** with $Fe(bpy)_3^{3+}$ (bpy = 2,2′-bipyridine)[26] exhibits broad absorption around 500–820 nm (Figure 3b). The absorption coefficient determined at 650 nm in PhCN was 13000 M^{-1} cm^{-1}. The characteristic features of $^1(ZnP)_3^*$, $^3(ZnP)_3^*$, and $(ZnP)_3^{\bullet+}$ described above are easily detectable markers for following intramolecular ET reactions.

Fc-(ZnP)$_3$: Nanosecond time-resolved absorption spectra of **Fc-(ZnP)$_3$** were measured (Figure 4). **Fc-(ZnP)$_3$** was excited at 532 nm, where the porphyrin moiety absorbs light exclusively. The differential spectrum recorded 250 ns after the laser pulse is characterized by bleaching of the porphyrin Q-band absorption around 600–800 nm. As time elapses, only the triplet–triplet absorption due to $^3(ZnP)_3^*$ is observed. This indicates little occurrence of photoinduced electron transfer from Fc to $^1(ZnP)_3^*$.

(ZnP)$_3$-C$_{60}$: Time-resolved transient absorption spectra of **(ZnP)$_3$-C$_{60}$** were also measured by pico- and nanosecond laser photolysis. In its picosecond time-resolved absorption

Table 2. ET rate constants (k_{ET}), quantum yields (Φ), and driving forces ($-\Delta G^0_{ET}$) in **(ZnP)$_3$-C$_{60}$**.

Solvent	Initial state[a]	Final state[a]	$-\Delta G^0_{ET}$ [eV]	k_{ET} [s^{-1}][b]	Φ[c]
PhCN (ε_s = 25.2)	^{1}**(ZnP)$_3^*$-C$_{60}$** (1.95 eV)	**(ZnP)$_3^{\bullet+}$-C$_{60}^{\bullet-}$** (1.36 eV)	0.59	$k_{ET(CS1)} = 2.8\times10^9$	$\Phi_{CS1}(^1ZnP^*) = 0.82$
	^{3}**(ZnP)$_3^*$-C$_{60}$** (1.56 eV)	**(ZnP)$_3^{\bullet+}$-C$_{60}^{\bullet-}$** (1.36 eV)	0.20	$k_{ET(CS3)} = 2.5\times10^7$	$\Phi_{CS3}(^3ZnP^*) = 1.0$
	(ZnP)$_3^{\bullet+}$-C$_{60}^{\bullet-}$ (1.36 eV)	**(ZnP)$_3$-C$_{60}$**	1.36	$k_{ET(CR1)} = 1.5\times10^6$	
THF(ε_s = 7.58)	^{1}**(ZnP)$_3^*$-C$_{60}$** (1.99 eV)	**(ZnP)$_3^{\bullet+}$-C$_{60}^{\bullet-}$** (1.35 eV)	0.64	$k_{ET(CS1)} = 3.9\times10^9$	$\Phi_{CS1}(^1ZnP^*) = 0.86$
	^{3}**(ZnP)$_3^*$-C$_{60}$** (1.56 eV)	**(ZnP)$_3^{\bullet+}$-C$_{60}^{\bullet-}$** (1.35 eV)	0.21	$k_{ET(CS3)} = 1.3\times10^7$	$\Phi_{CS3}(^3ZnP^*) = 1.0$
	(ZnP)$_3^{\bullet+}$-C$_{60}^{\bullet-}$ (1.35 eV)	**(ZnP)$_3$-C$_{60}$**	1.35	$k_{ET(CR1)} = 1.0\times10^6$	
DMF(ε_s = 36.7)	^{1}**(ZnP)$_3^*$-C$_{60}$** (1.97 eV)	**(ZnP)$_3^{\bullet+}$-C$_{60}^{\bullet-}$** (1.25 eV)	0.72	$k_{ET(CS1)} = 3.1\times10^9$	$\Phi_{CS1}(^1ZnP^*) = 0.84$
	^{3}**(ZnP)$_3^*$-C$_{60}$** (1.56 eV)	**(ZnP)$_3^{\bullet+}$-C$_{60}^{\bullet-}$** (1.25 eV)	0.31	$k_{ET(CS3)} = 7.3\times10^7$	$\Phi_{CS3}(^3ZnP^*) = 1.0$
	(ZnP)$_3^{\bullet+}$-C$_{60}^{\bullet-}$ (1.25 eV)	**(ZnP)$_3$-C$_{60}$**	1.25	$k_{ET(CR1)} = 1.3\times10^6$	

[a] The energy of each state relative to the ground state is given in parentheses. [b] The k_{ET} values for ET from $^1(ZnP)_3^*$ to C_{60} were determined from the fluorescence lifetimes by using the equation: $k_{ET} = [1/\tau(\textbf{(ZnP)$_3$-C$_{60}$})] - [1/\tau(\textbf{(ZnP)$_3$-ref})]$. The k_{ET} values for ET from $^3(ZnP)_3^*$ to C_{60} were determined from the rise component at 1000 nm. The k_{ET} values for CR were determined by analyzing the decay of $C_{60}^{\bullet-}$ at 1000 nm. [c] The efficiency (Φ) for charge separation was estimated on the basis of Figure 5.

Table 3. ET rate constants (k_{ET}), quantum yields (Φ) and the driving forces ($-\Delta G^0_{ET}$) in **Fc-(ZnP)$_3$-C$_{60}$**.

Solvent	Initial state[a]	Final state[a]	$-\Delta G^0_{ET}$ [eV^{-1}]	k_{ET} [s^{-1}][b]	Φ[c]
PhCN (ε_s = 25.2 eV)	**Fc-^{1}(ZnP)$_3^*$-C$_{60}$** (1.95 eV)	**Fc-(ZnP)$_3^{\cdot+}$-C$_{60}^{\cdot-}$** (1.36 eV)	0.59	$k_{ET(CS1)} = 2.7\times10^9$	$\Phi_{CS1}(^1ZnP^*) = 0.81$
	Fc-^{1}(ZnP)$_3^*$-C$_{60}$ (1.95 eV)	**Fc$^+$-(ZnP)$_3^{\cdot-}$-C$_{60}$** (1.82 eV)	0.13	$k_{ET(CS2)} = 8.9\times10^7$	$\Phi_{CS2}(^1ZnP^*) = 0.03$
	Fc-^{3}(ZnP)$_3^*$-C$_{60}$ (1.56 eV)	**Fc-(ZnP)$_3^{\cdot+}$-C$_{60}^{\cdot-}$** (1.36 eV)	0.20	$k_{ET(CS3)} = 2.5\times10^7$	$\Phi_{CS3}(^3ZnP^*) = 1.0$
	Fc-(ZnP)$_3^{\cdot+}$-C$_{60}^{\cdot-}$ (1.36 eV)	**Fc$^+$-(ZnP)$_3$-C$_{60}^{\cdot-}$** (1.03 eV)	0.33	$k_{ET(CSH1)} = 5.2\times10^6$	$\Phi_{CSH1} = 0.78$
	Fc-(ZnP)$_3^{\cdot+}$-C$_{60}^{\cdot-}$ (1.36 eV)	**Fc-(ZnP)$_3$-C$_{60}$**	1.36	$k_{ET(CR1)} = 1.5\times10^6$	
	Fc$^+$-(ZnP)$_3$-C$_{60}^{\cdot-}$ (1.03 eV)	**Fc-(ZnP)$_3$-C$_{60}$**	1.03	$k_{ET(CR2)} = 2.9$[d]	Φ_{CS}(total) = 0.82(0.83)[f]
THF (ε_s = 7.58)	**Fc-^{1}(ZnP)$_3^*$-C$_{60}$** (1.99 eV)	**Fc-(ZnP)$_3^{\cdot+}$-C$_{60}^{\cdot-}$** (1.35 eV)	0.64	$k_{ET(CS1)} = 2.6\times10^9$	$\Phi_{CS1}(^1ZnP^*) = 0.80$
	Fc-^{1}(ZnP)$_3^*$-C$_{60}$ (1.99 eV)	**Fc$^+$-(ZnP)$_3^{\cdot-}$-C$_{60}$** (1.94 eV)	0.05	$k_{ET(CS2)} = 4.2\times10^7$	$\Phi_{CS2}(^1ZnP^*) = 0.01$
	Fc-^{3}(ZnP)$_3^*$-C$_{60}$ (1.56 eV)	**Fc-(ZnP)$_3^{\cdot+}$-C$_{60}^{\cdot-}$** (1.35 eV)	0.21	$k_{ET(CS3)} = 1.3\times10^7$	$\Phi_{CS3}(^3ZnP^*) = 1.0$
	Fc-(ZnP)$_3^{\cdot+}$-C$_{60}^{\cdot-}$ (1.35 eV)	**Fc$^+$-(ZnP)$_3$-C$_{60}^{\cdot-}$** (1.00 eV)	0.35	$k_{ET(CSH1)} = 3.7\times10^6$	$\Phi_{CSH1} = 0.79$
	Fc-(ZnP)$_3^{\cdot+}$-C$_{60}^{\cdot-}$ (1.35 eV)	**Fc-(ZnP)$_3$-C$_{60}$**	1.35	$k_{ET(CR1)} = 1.0\times10^6$	
	Fc$^+$-(ZnP)$_3$-C$_{60}^{\cdot-}$ (1.00 eV)	**Fc-(ZnP)$_3$-C$_{60}$**	1.00	[e]	Φ_{CS}(total) = 0.83
DMF (ε_s = 36.7)	**Fc-^{1}(ZnP)$_3^*$-C$_{60}$** (1.97 eV)	**Fc-(ZnP)$_3^{\cdot+}$-C$_{60}^{\cdot-}$** (1.25 eV)	0.72	$k_{ET(CS1)} = 3.0\times10^9$	$\Phi_{CS1}(^1ZnP^*) = 0.84$
	Fc-^{1}(ZnP)$_3^*$-C$_{60}$ (1.97 eV)	**Fc$^+$-(ZnP)$_3^{\cdot-}$-C$_{60}$** (1.93 eV)	0.04	$k_{ET(CS2)} = 1.8\times10^8$	$\Phi_{CS2}(^1ZnP^*) = 0.05$
	Fc-^{3}(ZnP)$_3^*$-C$_{60}$ (1.56 eV)	**Fc-(ZnP)$_3^{\cdot+}$-C$_{60}^{\cdot-}$** (1.25 eV)	0.31	$k_{ET(CS3)} = 7.3\times10^7$	$\Phi_{CS3}(^3ZnP^*) = 1.0$
	Fc-(ZnP)$_3^{\cdot+}$-C$_{60}^{\cdot-}$ (1.25 eV)	**Fc$^+$-(ZnP)$_3$-C$_{60}^{\cdot-}$** (0.91 eV)	0.34	$k_{ET(CSH1)} = 4.1\times10^6$	$\Phi_{CSH1} = 0.76$
	Fc-(ZnP)$_3^{\cdot+}$-C$_{60}^{\cdot-}$ (1.25 eV)	**Fc-(ZnP)$_3$-C$_{60}$**	1.25	$k_{ET(CR1)} = 1.3\times10^6$	
	Fc$^+$-(ZnP)$_3$-C$_{60}^{\cdot-}$ (0.91 eV)	**Fc-(ZnP)$_3$-C$_{60}$**	0.91	$k_{ET(CR2)} = 1.9$[d]	Φ_{CS}(total) = 0.80

[a] The energy of each state relative to the ground state is given in parentheses. [b] The $k_{ET(CS)}$ values for ET from $^1(ZnP)_3^*$ to C_{60} and Fc to $^1(ZnP)_3^*$ were determined from the fluorescence lifetimes by using the equations $k_{ET(CS1)} = [1/\tau(\textbf{Fc-(ZnP)$_3$-C$_{60}$})]-[1/\tau(\textbf{Fc-(ZnP)$_3$})]$ and $k_{ET(CS2)} = [1/\tau(\textbf{Fc-(ZnP)$_3$})]-[1/\tau(\textbf{(ZnP)$_3$-ref})]$. The $k_{ET(CS3)}$ values are assumed to be the same as those of **(ZnP)$_3$-C$_{60}$**. The $k_{ET(CSH1)}$ values were determined from the decay rate constants of $(ZnP)_3^{\cdot+}$ for **Fc-(ZnP)$_3$-C$_{60}$**, referred to those of **(ZnP)$_3$-C$_{60}$**. The $k_{ET(CR2)}$ values were determined by analyzing the decay of the ESR signal due to $C_{60}^{\cdot-}$. [c] The efficiencies (Φ) for each deactivation pathway were estimated on the basis of Figure 7. [d] At 163 K. [e] Not measured. [f] Quantum yield obtained from the comparative method.

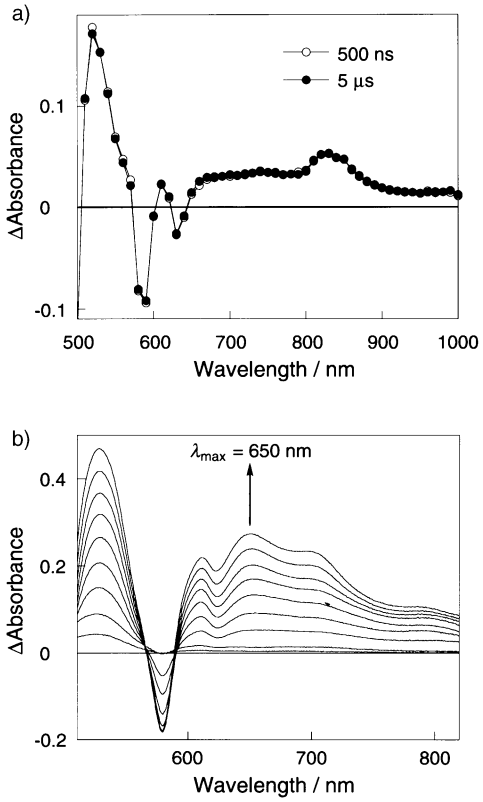

Figure 3. a) Differential absorption spectra obtained upon nanosecond laser flash photolysis (532 nm) of 0.1 mM of **(ZnP)$_3$-ref** solution in argon-saturated PhCN with a time delay of 500 ns and 5 µs. b) Spectral change upon addition of $[Fe(bpy)_3]^{3+}$ (0.11, 0.22, 0.33, 0.44, 0.56, 0.67, 0.78, 0.89, 1.0 equiv) to a PhCN solution containing **(ZnP)$_3$-ref** (2.0×10^{-5} M).

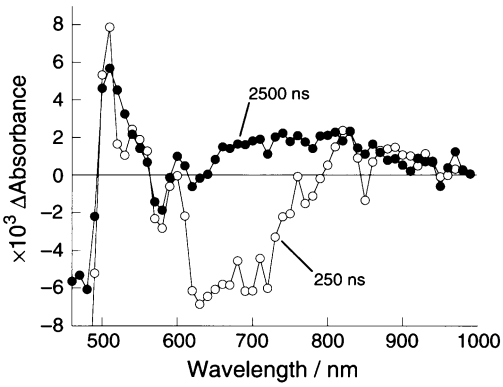

Figure 4. Nanosecond time-resolved absorption spectra of **Fc-(ZnP)$_3$** (0.1 mM) in argon-saturated PhCN excited at 532 nm with a time delay of 250 ns (open rings) and 2500 ns (solid rings).

spectrum in PhCN (Figure 2), **(ZnP)$_3$-C$_{60}$** was excited at 560 nm, where the porphyrin moiety absorbs light exclusively. The differential spectrum taken immediately after the laser pulse is characterized by bleaching of the porphyrin Q-band absorption at 580 nm due to the $^1(ZnP)_3^*$. As time elapses, a new transition around 1000 nm appears, accompanied by another new broad absorption around 600–700 nm (the solid line in Figure 2), which is quite different from the spectral features of $^3(ZnP)_3^*$ in Figures 3a and 4. By comparison with the absorption of $C_{60}^{\cdot-}$ and $(ZnP)_3^{\cdot+}$ (vide supra), we ascribe the former and the latter bands to the $C_{60}^{\cdot-}$ moiety[27] and the $(ZnP)_3^{\cdot+}$ moiety, respectively. This indicates the occurrence of a photoinduced ET, evolving from $^1(ZnP)_3^*$ to C_{60} and, in turn, creating the **(ZnP)$_3^{\cdot+}$-C$_{60}^{\cdot-}$** state. The energy levels in PhCN, as extracted from Table 2 into Figure 5 to illustrate the relaxation pathways of photoexcited **(ZnP)$_3$-C$_{60}$**. Similar transient absorption spectra, specifically the spectral fingerprints of $(ZnP)_3^{\cdot+}$ and $C_{60}^{\cdot-}$, were obtained in THF and DMF.

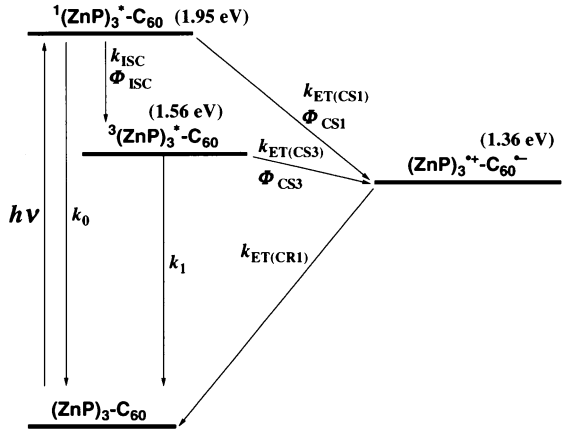

Figure 5. Reaction scheme and energy diagram for **(ZnP)$_3$-C$_{60}$** in PhCN.

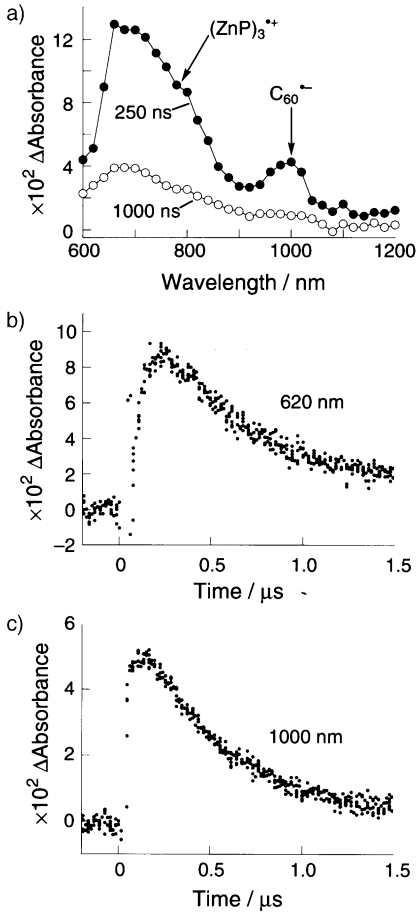

Figure 6. a) Nanosecond time-resolved absorption spectra of **(ZnP)$_3$-C$_{60}$** (0.1 mM) in argon-saturated PhCN excited at 532 nm with a time delay of 250 ns (open rings) and 1000 ns (solid rings). Time profiles of absorbance at b) 620 nm and c) 1000 nm.

The fluorescence lifetimes τ of **(ZnP)$_3$-C$_{60}$** and **(ZnP)$_3$-ref** were also measured with a time-correlated single-photon-counting apparatus using 400 nm excitation, where the porphyrin moiety absorbs light exclusively. The fluorescence decay was monitored at 630 nm, for the emission from only the porphyrin moiety. No emission from the C_{60} moiety was detected for **(ZnP)$_3$-C$_{60}$**, even at 720 nm.[24] In general, the fluorescence decay curves were fitted well by a single exponential decay component. The fluorescence lifetimes τ are listed in Table 4. On the basis of the fluorescence lifetimes

Table 4. Fluorescence lifetimes (τ) of **Fc-(ZnP)$_3$-C$_{60}$** and the reference compounds in THF, PhCN, and DMF.[a]

Compound	Fluorescence lifetime τ [ps]		
	PhCN (ε_s = 25.2)	THF (ε_s = 7.58)	DMF (ε_s = 36.7)
(ZnP)$_3$-C$_{60}$	290	220	270
(ZnP)$_3$-ref	1600	1600	1700
Fc-(ZnP)$_3$-C$_{60}$	300	310	280
Fc-(ZnP)$_3$	1400	1500	1300

[a] Excitation wavelength = 400 nm, monitoring wavelength = 630 nm.

(λ_{obs} = 630 nm) in PhCN, the ET rate constants were determined: $k_{ET(CS1)} = 2.8\times10^9\ s^{-1}$ for ET from ^{1}ZnP* to C_{60} with quantum efficiency $\Phi_{CS1}(^1ZnP^*) = k_{ET(CS1)}/(k_{ET(CS1)} + k_{ISC} + k_0) = 0.82$. Similar $k_{ET(CS1)}$ values were also determined: $k_{ET(CS1)} = 3.9\times10^9\ s^{-1}$ in THF and $3.1\times10^9\ s^{-1}$ in DMF (Table 2). These results are similar to those for the corresponding references, **ZnP-C$_{60}$** ($k_{ET(CS1)} = 9.5\times10^9\ s^{-1}$)[19] and **(ZnP)$_2$-C$_{60}$** ($k_{ET(CS1)} = 6.6\times10^9\ s^{-1}$)[18] in Scheme 1.

Formation of $C_{60}^{\bullet-}$ (1000 nm) and $(ZnP)_3^{\bullet+}$ (broad absorption around 600–700 nm) was further substantiated (Figure 6) by a set of complementary nanosecond laser experiments using 532 nm excitation, where the porphyrin moiety absorbs light exclusively. The transient absorption spectrum obtained for **(ZnP)$_3$-C$_{60}$** (Figure 6) matches the spectrum in Figure 2, corroborating the formation of $C_{60}^{\bullet-}$ and $(ZnP)_3^{\bullet+}$ well. The resulting charge-separated state recombines to regenerate the singlet ground state. From the decay kinetics at 1000 nm and 620 nm the rate constant $k_{ET(CR1)} = 1.5\times10^6\ s^{-1}$ deduced for a PhCN solution was virtually the same as those of the corresponding references: **ZnP-C$_{60}$** ($k_{ET(CR1)} = 1.3\times10^6\ s^{-1}$)[19] and **(ZnP)$_2$-C$_{60}$** ($k_{ET(CR1)} = 1.9\times10^6\ s^{-1}$).[18] This indicates that the charge recombination from the $C_{60}^{\bullet-}$ moiety to the porphyrin moiety adjacent to the $C_{60}^{\bullet-}$ is the rate-determining step. The time profiles of absorbance at 620 nm and 1000 nm display rise components with identical rate constants of $2.5\times10^7\ s^{-1}$ before the decay of the characteristic bands due to **(ZnP)$_3^{\bullet+}$-C$_{60}^{\bullet-}$**. The unquenched porphyrin trimer singlet excited state undergoes intersystem crossing to yield the corresponding triplet excited state, which results in the quantitative formation of **(ZnP)$_3^{\bullet+}$-C$_{60}^{\bullet-}$** by photoinduced ET ($\Phi_{CS3}(^3ZnP^*) = k_{ET(CS3)}/(k_{ET(CS3)} + k_1) = 1.0$). In other words, excitation of **(ZnP)$_3$-C$_{60}$** leads to the exclusive formation of the **(ZnP)$_3^{\bullet+}$-C$_{60}^{\bullet-}$** state via $^1(ZnP)_3^*$ and $^3(ZnP)_3^*$.

The photodynamic behavior of **(ZnP)$_3$-C$_{60}$** in THF and DMF is similar to that described in PhCN (Table 2). A possible explanation for this analogy is based on the corresponding energy levels. In particular, the energies of the excited states ($^1(ZnP)_3^*$ 1.95–1.99 eV, $^3(ZnP)_3^*$ 1.56 eV, $^1C_{60}^*$ 1.75 eV, $^3C_{60}^*$ 1.50 eV) are substantially higher than the energy of the charge-separated state in PhCN (1.36 eV), THF (1.35 eV), and DMF (1.25 eV). This, in turn, guaran-

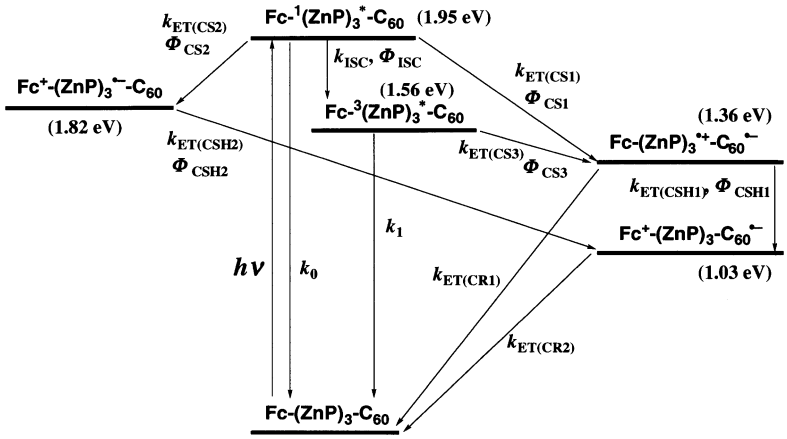

Figure 7. Reaction scheme and energy diagram for **Fc-(ZnP)$_3$-C$_{60}$** in PhCN.

tees large driving forces for the associated charge separation and CR processes.

Fc-(ZnP)$_3$-C$_{60}$: The energy levels in PhCN, which are expected to be of significance for the photoinduced ET reactions in **Fc-(ZnP)$_3$-C$_{60}$**, are taken from the data summarized in Table 3 and displayed in Figure 7. Since a ferrocene unit is tethered at the end of **(ZnP)$_3$-C$_{60}$**, the pentad will display coupled photoinduced ET: **Fc-^{1}(ZnP)$_3^*$-C$_{60}$** (1.95 eV)→**Fc-(ZnP)$_3^{\bullet+}$-C$_{60}^{\bullet-}$** (1.36 eV)→**Fc$^+$-(ZnP)$_3$-C$_{60}^{\bullet-}$** (1.03 eV) in PhCN (Figure 7).

Its picosecond time-resolved absorption spectra in PhCN after a laser pulse (560 nm) demonstrate that the spectral behavior of **Fc-(ZnP)$_3$-C$_{60}$** is similar to that of **(ZnP)$_3$-C$_{60}$** (Figure 2). This clearly shows that initial ET occurs from the ^{1}(ZnP)$_3^*$ to the C$_{60}$ moiety to generate **Fc-(ZnP)$_3^{\bullet+}$-C$_{60}^{\bullet-}$**. The rate constant ($k_{ET(CS1)} = 2.7\times10^9\ s^{-1}$) and the efficiency of the formation of **Fc-(ZnP)$_3^{\bullet+}$-C$_{60}^{\bullet-}$** from ^{1}(ZnP)$_3^*$ [$\Phi_{CS1}(^1ZnP^*) = 0.81$] were determined as described for **(ZnP)$_3$-C$_{60}$** (Table 3). The fluorescence lifetime of **Fc-(ZnP)$_3$** indicates that photoinduced ET also takes place from the Fc to the ^{1}(ZnP)$_3^*$ to produce **Fc$^+$-(ZnP)$_3^{\bullet-}$** (Table 4). However, the ET from the Fc to the ^{1}(ZnP)$_3^*$ [$k_{ET(CS2)} = 8.9\times10^7\ s^{-1}$] is much slower (by a factor of $^1/_{29}$) than that from ^{1}(ZnP)$_3^*$ to C$_{60}$. Thus, the deactivation pathway to generate **Fc$^+$-(ZnP)$_3^{\bullet-}$-C$_{60}$** is quite negligible [$\Phi_{CS2}(^1ZnP^*) = 0.03$], although the charge-separated state would undergo charge shift (CSH) ($-\Delta G^0_{ET(CSH2)} = 0.79$ eV) to the C$_{60}$ moiety to generate **Fc$^+$-(ZnP)$_3$-C$_{60}^{\bullet-}$** efficiently.

Nanosecond transient absorption spectra of **Fc-(ZnP)$_3$-C$_{60}$** at a time delay in the nano- and microsecond regions also exhibit formation of C$_{60}^{\bullet-}$ around 1000 nm, whereas the transient absorption due to the (ZnP)$_3^{\bullet+}$ around 600–700 nm disappears (Figure 8a), in contrast with the case of **(ZnP)$_3$-C$_{60}$** (Figure 6a). The resultant absorption spectrum is virtually identical to those of **Fc$^+$-ZnP-C$_{60}^{\bullet-}$**[19] and **Fc$^+$-(ZnP)$_2$-C$_{60}^{\bullet-}$**.[18] Taking into account the small molar absorption coefficient of the ferricenium ion ($\varepsilon\approx1000\ M^{-1}\,cm^{-1}$ at 800 nm),[28] one can conclude that the resulting charge-separated state (**Fc-(ZnP)$_3^{\bullet+}$-C$_{60}^{\bullet-}$**) undergoes the CSH from the Fc moiety to the (ZnP)$_3^{\bullet+}$ moiety to generate **Fc$^+$-(ZnP)$_3$-C$_{60}^{\bullet-}$**. The time profile of absorption around 650 nm can be fitted by a fast decay [τ((ZnP)$_3^{\bullet+}$) = 150 ns] and slow decay identified as the absorption of C$_{60}^{\bullet-}$ in **Fc$^+$-(ZnP)$_3$-C$_{60}^{\bullet-}$** (Figure 8b). The fast decay component corresponds to the sum of the CSH from the Fc moiety to the (ZnP)$_3^{\bullet+}$ and the CR from the C$_{60}^{\bullet-}$ to the (ZnP)$_3^{\bullet+}$. Given that the $k_{ET(CR1)}$ of **Fc-(ZnP)$_3^{\bullet+}$-C$_{60}^{\bullet-}$** is the same as that of **(ZnP)$_3^{\bullet+}$-C$_{60}^{\bullet-}$** ($1.5\times10^6\ s^{-1}$), the $k_{ET(CSH1)}$ and the quantum yield of CSH

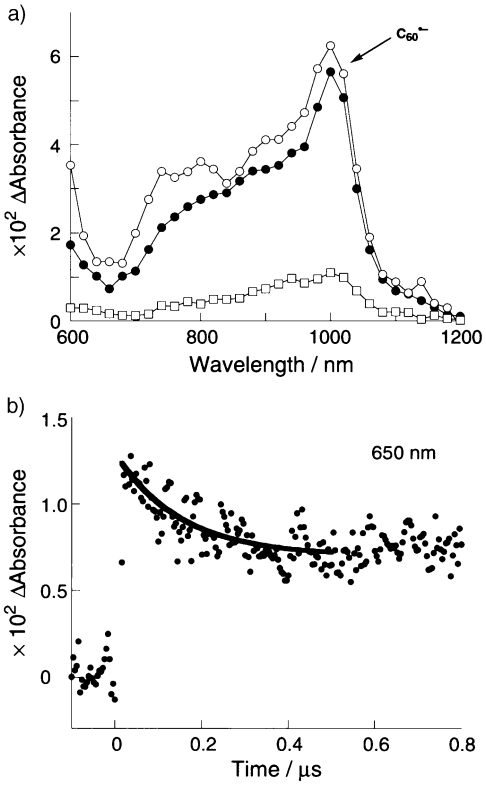

Figure 8. a) Nanosecond time-resolved absorption spectra of **Fc-(ZnP)$_3$-C$_{60}$** (0.1 mM) in argon-saturated PhCN excited at 532 nm with a time delay of 500 ns (open rings), 15 μs (solid rings), and 150 μs (open squares). b) Time profile of absorbance at 650 nm.

(Φ_{CSH1}), determined according to Equation (3), are $5.2\times10^6\ s^{-1}$ and 0.78.

$$\Phi_{CSH1} = \frac{k_{ET(CSH1)}}{k_{ET(CSH1)} + k_{ET(CR1)}} \quad (3)$$

It is interesting that the CSH value is smaller by two orders of magnitude than that of **Fc-ZnP-C$_{60}$** ($2.8\times10^9\ s^{-1}$), and is also smaller by a factor of $^1/_2$ than that of **Fc-(ZnP)$_2$-C$_{60}$**.[18] The relatively slow CSH of **Fc-(ZnP)$_3$-C$_{60}$** may be ascribed to the slow charge migration in the porphyrin trimer

in comparison with that in **Fc-ZnP-C_{60}** and **Fc-$(ZnP)_2$-C_{60}** (vide infra).

On the basis of the predominant excitation of the ZnP moiety (>99%), the total quantum yield (Φ_{CS}(total)) for CS is 0.83 when determined by applying the comparative method from the nanosecond time-resolved transient spectra (monofunctionalized $C_{60}^{\bullet-}$, $\varepsilon_{1000\,nm} = 4700\,M^{-1}\,cm^{-1}$).[27b] That the quantum yield is greater than those for **Fc^+-ZnP-H_2P-$C_{60}^{\bullet-}$** (0.17–0.24)[13] can be rationalized by the higher efficiency of the CSH along the *meso*,*meso*-linked zinc porphyrin arrays than that of the CSH in **Fc-ZnP-H_2P-C_{60}**. Since the unquenched porphyrin singlet excited state undergoes intersystem crossing to yield the porphyrin triplet excited state, photoinduced ET from the porphyrin triplet excited state to the C_{60} moiety ($k_{ET(CS3)}$) may occur to produce the charge-separated state, as in the case of **$(ZnP)_3$-C_{60}** (vide supra). Assuming that 1) the quantum yield of CSH from **Fc^+-$(ZnP)_3^{\bullet-}$-C_{60}** to **Fc^+-$(ZnP)_3$-$C_{60}^{\bullet-}$** is unity ($\Phi_{CSH2} = 1$), 2) the decay of **Fc-^{1}$(ZnP)_3^*$-C_{60}** to the ground state is negligible ($\Phi_{k_0} \approx 0$), and 3) the $k_{ET(CS3)}$ value is the same as that of **$(ZnP)_3$-C_{60}**, the total quantum yield of the charge separation [Φ_{CS}(total) = $\Phi_{CS1}\times\Phi_{CSH1} + \Phi_{CS2}\times\Phi_{CSH2} + \Phi_{ISC}\times\Phi_{CS3}\times\Phi_{CSH1}$] is found to be 0.82, which agrees well with the quantum yield obtained from the transient absorption spectra (Table 3). Similar photodynamic behavior was observed in THF (Φ_{CS}(total) = 0.83) and DMF (Φ_{CS}(total) = 0.80); the results are summarized in Table 3. The overall quantum yields of formation of **Fc^+-$(ZnP)_3$-$C_{60}^{\bullet-}$** are as high as those of **Fc^+-$(ZnP)_2$-$C_{60}^{\bullet-}$** (0.82–0.92),[29] despite the larger R_{ee} value in the former.

In contrast to the previously reported tetrad **Fc-$(ZnP)_2$-C_{60}**, the decay dynamics of the charge-separated radical ion pair [**Fc^+-$(ZnP)_3$-$C_{60}^{\bullet-}$**] does not obey first-order kinetics (Figure 9a). Instead, the time profiles at 1000 nm (that is, at the maximum of the $C_{60}^{\bullet-}$ absorption) obey second-order kinetics, as shown in Figure 9b, where [**Fc^+-$(ZnP)_3$-$C_{60}^{\bullet-}$**]$^{-1}$ is plotted against time. From the slope of the linear plot is obtained the second-order rate constant of $2.7\times10^9\,M^{-1}s^{-1}$, which is nearly completely diffusion-controlled. The second-order rate law was further verified by changing the effective radical ion pair concentration obtained by employing different laser power levels over a wide range (with increments reaching a five-fold increase in laser intensity). The preference for such an intermolecular ET (second-order kinetics) over an intramolecular ET (first-order kinetics) indicates that the *intra*molecular charge recombination from the $C_{60}^{\bullet-}$ to the Fc^+ moiety is too slow to compete with the *inter*molecular ET.

ESR measurements under photoirradiation: To segregate the *inter*molecular ET from the *intra*molecular ET process in **Fc^+-$(ZnP)_3$-$C_{60}^{\bullet-}$**, ESR measurements were performed in frozen PhCN or DMF using a low concentration of **Fc-$(ZnP)_3$-C_{60}** (1.0×10^{-5} M) under photoirradiation. The ESR spectrum in frozen DMF (Figure 10a) under irradiation at

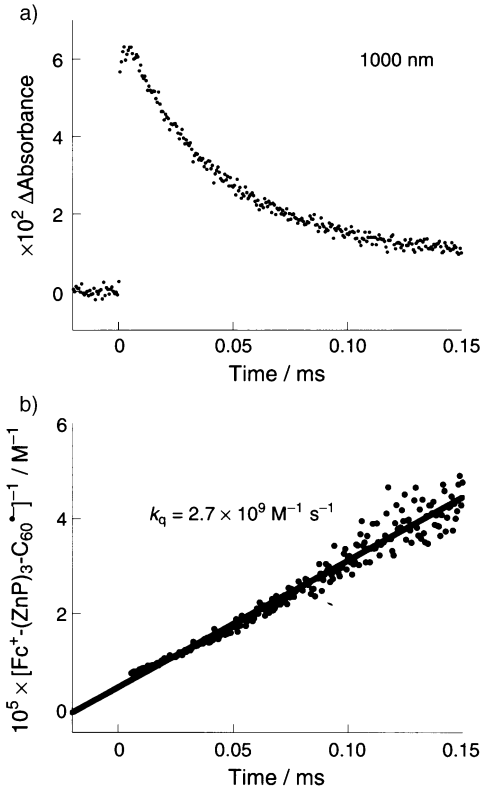

Figure 9. a) Time profiles of absorbance at 1000 nm for **Fc-$(ZnP)_3$-C_{60}** (0.1 mM) in argon-saturated PhCN excited at 532 nm. b) Second-order plot derived from the absorption change at 1000 nm.

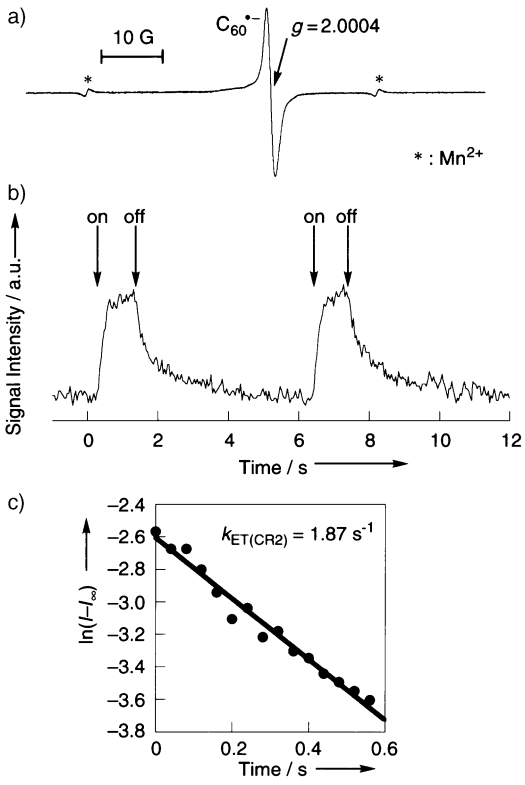

Figure 10. a) ESR spectrum of **Fc-$(ZnP)_3$-C_{60}** (1.0×10^{-5} M) in frozen deaerated DMF observed at 163 K under UV/Vis photoirradiation with a high-pressure Hg lamp. b) Signal intensity response of **Fc-$(ZnP)_3$-C_{60}** in frozen deaerated DMF at the ESR signal intensity maximum due to the $C_{60}^{\bullet-}$. c) First-order plot for the decay of the ESR signal intensity in **Fc-$(ZnP)_3$-C_{60}** ($k_{ET(CR2)} = 1.87\,s^{-1}$).

163 K shows a characteristic broad signal attributable to $C_{60}^{\bullet-}$ ($g = 2.0004$).[30] $C_{60}^{\bullet-}$ was also produced by chemical reduction of **C_{60}-ref** with tetramethylsemiquinone radical anion, yielding a virtually identical ESR signal. The lack of direct ESR evidence for the ferricenium ion (Fc^+) in the **Fc^+-$(ZnP)_3$-$C_{60}^{\bullet-}$** radical ion pair is rationalized in terms of the well-known line broadening of the Fc^+ ESR signal.[31] Similar ESR spectra were observed for **Fc-$(ZnP)_3$-C_{60}** in frozen PhCN.

The ESR signal in a fixed magnetic field was monitored to obtain maximal intensity of the $C_{60}^{\bullet-}$ response and to enable performance of the following lifetime experiments in frozen DMF. As shown in Figure 10b, the ESR signal grows immediately when the photoirradiation of **Fc-$(ZnP)_3$-C_{60}** is "turned on". When the source was "turned off", the ESR signal did not diminish instantly. Instead, it exhibited a slow decay that lasted nearly for seconds, which was best fitted by first-order kinetics yielding a rate constant of $1.9\ s^{-1}$ (Figure 10c) for the *intra*molecular CR process ($k_{ET(CR2)}$). The clean mono-exponential dynamics corroborate the origin of the ESR signal to be indeed the *intra*molecular radical ion pair (**Fc^+-$(ZnP)_3$-$C_{60}^{\bullet-}$**). In contrast, as it may prevail between radical ion pairs located in close proximity, an intermolecular ET should exhibit multi-exponential decay profiles, depending on the relative distance between the radical ion pairs. Under the present experimental conditions this contribution was found to be negligible. The $k_{ET(CR2)}$ value is also $2.9\ s^{-1}$ when determined in frozen PhCN at 163 K.

To shed light on the extremely slow charge recombination, the structure of the *meso,meso*-linked porphyrin trimer radical cation is optimized by B3LYP calculation with the LanL2MB basis set. The three porphyrin rings are found to be perpendicular each other, minimizing the delocalization of excess spin over the *meso,meso*-linked array (Figure 11).

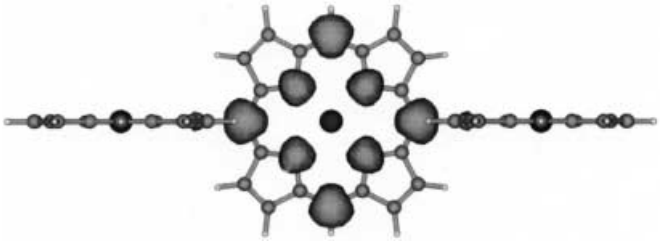

Figure 11. Optimized structure and spin density distribution of *meso,meso*-linked porphyrin trimer radical cation. The optimized structure is obtained by B3LYP calculation with the LanL2MB basis set.

The excess spin is localized mainly on the middle porphyrin of the three.[32] Thus, the observed high quantum yield of radical ion pair formation results from efficient charge separation through the porphyrin trimer,[14],[15] whereas the slow charge recombination is associated with the localized porphyrin radical cation in the porphyrin trimer.

Conclusion

The present study has demonstrated unequivocally occurrence of an *intra*molecular CR process in the **Fc-$(ZnP)_3$-C_{60}** pentad, observable by ESR measurements under photoirradiation. More importantly, the lifetime (0.53 s in frozen DMF and 0.34 s in frozen PhCN at 163 K) is one of the longest ever reported for *intra*molecular CR in a donor–acceptor ensemble.[13],[33–35] The lifetime is comparable with that ($\approx$1 s) of the bacteriochlorophyll dimer radical cation [$(Bchl)_2^{\bullet+}$]–secondary quinone radical anion ($Q_B^{\bullet-}$) ion pair in bacterial photosynthetic reaction centers.[1],[2] Such an extremely long lifetime of a charge-separated state could only be determined in frozen media, since in solution *inter*molecular dynamics dominate the back ET. It should be emphasized that efficient formation of the final charge-separated state with a high quantum yield ($\Phi = 0.83$) is also achieved in the present pentad system. Such excellent performance of this system can be rationalized by the efficient charge separation and retarded charge recombination through the *meso,meso*-linked porphyrin trimer.

Experimental Section

General: Melting points were recorded on a Yanagimoto micro-melting point apparatus and not corrected. ^{1}H NMR spectra were measured on a JEOL EX-270 and JEOL JNM-AL300. Fast atom bombardment mass spectra (FAB MS) were obtained on a JEOL JMS-DX300. Matrix-assisted laser desorption/ionization (MALDI) time-of-flight mass spectra (TOF) were measured on a Kratos Compact MALDI I (Shimadzu). IR spectra were measured on a Shimadzu FT-IR 8200 PC using KBr disks. Steady-state absorption spectra in the visible and near-IR regions were measured on a Shimadzu UV-3100PC. The edge-to-edge distances (R_{ee}) were determined from CPK modeling using CAChe (version 3.7, CAChe Scientific, 1994).

Materials: All solvents and chemicals were of reagent grade quality, obtained commercially and used without further purification except as noted below. The tetrabutylammonium hexafluorophosphate used as a supporting electrolyte for the electrochemical measurements was obtained from Tokyo Kasei Organic Chemicals. Tris(2,2′-bipyridine)iron(II) complex was prepared by adding 2,2′-bipyridine (3 equiv) to an aqueous solution of ferrous sulfate.[26] Tris(2,2′-bipyridine)iron(III) hexafluorophosphate, $[Fe(bpy)_3](PF_6)_3$, was prepared by oxidation of the corresponding iron(II) complex with lead dioxide in aqueous H_2SO_4 followed by the addition of KPF_6.[26] THF, PhCN, and DMF were purchased from Wako Pure Chemical Industries, Ltd., and purified by successive distillations over calcium hydride. Thin-layer chromatography (TLC) and flash column chromatography were performed with Art. 5554 DC-Alufolien Kieselgel 60 F_{254} (Merck) and Fujisilicia BW300, respectively.

Fc-$(ZnP)_3$-C_{60} (3): A solution of $AgPF_6$ (879.8 mg) in acetonitrile (11 mL) was added all at once to a solution of **1** (1232.2 mg, 1.39 mmol) and **2** (348.2 mg, 0.464 mmol) in dry $CHCl_3$ (250 mL) and dry *N,N*-dimethylacetamide (DMA) (3.8 mL). The reaction mixture was protected from light and stirred at 30 °C for 22 h. The reaction mixture was washed with water, it was dried over anhydrous Na_2SO_4, and then the solvent was evaporated. The reaction mixture was dissolved in a mixture of chloroform (250 mL), trifluoroacetic acid (100 mL) and 5% aqueous sulfuric acid (75 mL). After being stirred overnight, the mixture was poured into water (300 mL) and extracted with $CHCl_3$. The organic layer was washed with a saturated $NaHCO_3$ aqueous solution, dried over anhydrous Na_2SO_4, and evaporated. Flash column chromatography on silica gel with hexane–toluene (1:2) as an eluent ($R_f = 0.50$ in benzene) and subsequent gel permeation chromatography (BioRad Bio-Beads SX-1, toluene) gave **3** as a dark purple solid (55% yield, 445.6 mg, 0.192 mmol). M.p. > 300 °C; ^{1}H NMR (270 MHz, $CDCl_3$) δ = 8.96 (d, J = 5 Hz, 4H), 8.87 (d, J = 5 Hz, 4H), 8.69 (d, J = 5 Hz, 4H), 8.65 (d, J = 5 Hz, 4H), 8.49 (d, J = 8 Hz, 4H), 8.41 (d, J = 5 Hz, 4H), 8.21 (d, J = 5 Hz, 4H), 8.15 (d, J = 5 Hz, 4H), 8.09 (d, J = 2 Hz, 8H), 8.05 (d, J = 2 Hz, 4H), 7.73 (t, J = 2 Hz, 4H), 7.59 (t, J = 2 Hz, 2H), 4.14 (s,

6H), 1.46 (s, 72H), 1.34 (s, 36H), −1.60 (brs, 2H), −2.12 ppm (brs, 4H); MALDI-TOF MS (positive mode): *m/z*: 2325 [*M*+H$^+$]; FTIR (KBr): $\tilde{\nu}$= 3451, 3319, 2959, 2332, 1728, 1591, 1473, 1364, 1274, 1110, 962, 918, 796, 716 cm^{-1}.

Free-base porphyrin carboxylic acid 4: A mixture of **3** (345.5 mg, 0.149 mmol) in THF/ethanol (8:2, 350 mL) and aqueous KOH solution (2 M, 35 mL) was refluxed under nitrogen (1 atm) for 36 h. After cooling, the reaction mixture was diluted with water (300 mL), and the precipitate was filtered. Acidification (pH 1) of an aqueous suspension of the residue with aqueous HCl solution and subsequent filtration gave **4** as a black-brown solid (327.2 mg, 0.142 mmol, 96%). M.p. > 300 °C; ^{1}H NMR (270 MHz, $CDCl_3$/DMSO = 5:2): δ = 8.94 (d, J = 5 Hz, 4H), 8.90 (d, J = 5 Hz, 4H), 8.63 (d, J = 5 Hz, 4H), 8.48 (d, J = 8 Hz, 4H), 8.37 (d, J = 8 Hz, 4H), 8.07 (d, J = 5 Hz, 4H), 8.05 (d, J = 2 Hz, 8H), 7.71 (t, J = 2 Hz, 4H), 1.45 (s, 72H), −2.21 ppm (brs, 4H); MALDI-TOF MS (positive mode): *m/z*: 2298; FTIR (KBr): $\tilde{\nu}$=3318, 2962, 2363, 1739, 1592, 1474, 1361, 1247, 973, 916, 793, 716 cm^{-1}.

Ferrocene–*meso*,*meso*-linked porphyrin trimer 5: A solution of **4** (24.5 mg, 0.0108 mmol), pyridine (0.04 mL), and thionyl chloride (0.03 mL) in benzene (10 mL) was refluxed for 2.5 h. The excess thionyl chloride and solvents were removed under reduced pressure and the residue was redissolved in benzene (5 mL). This solution containing **4** was added to a stirred solution of 4-aminophenylferrocene (2.17 mg, 0.00783 mmol) and 2-(4-aminophenyl)-5,5-dimethyl-1,3-dioxane (2.88 mg, 0.0138 mmol) in benzene (2.5 mL) and pyridine (0.5 mL), and the solution was stirred for 16 h. TLC showed three products and the second (R_f = 0.15, chloroform) was separated by flash column chromatography. The second fraction was concentrated and dissolved in a mixture of chloroform (10 mL), trifluoroacetic acid (4 mL), and 5% aqueous sulfuric acid (3 mL). After being stirred for 17 h, the mixture was poured into 50 mL of water and extracted with $CHCl_3$. The organic layer was washed with saturated $NaHCO_3$ aqueous solution, dried over anhydrous Na_2SO_4, and evaporated. Flash column chromatography on silica gel with chloroform as an eluent (R_f = 0.15) and subsequent reprecipitation from chloroform/methanol gave **5** as a black-red solid (5.4 mg, 0.0020 mmol, 19%). M.p. > 300 °C; ^{1}H NMR (270 MHz, $CDCl_3$): δ = 10.04 (s, 1H), 8.98 (d, J = 5 Hz, 4H), 8.91 (d, J = 5 Hz, 2H), 8.89 (d, J = 5 Hz, 2H), 8.71 (d, J = 5 Hz, 4H), 8.66 (d, J = 5 Hz, 4H), 8.50 (d, J = 8 Hz, 2H), 8.48 (d, J = 8 Hz, 2H), 8.37 (d, J = 8 Hz, 2H), 8.35 (d, J = 8 Hz, 2H), 8.33 (brs., 1H), 8.22 (d, J = 5 Hz, 2H), 8.17 (brs, 1H), 8.16 (d, J = 5 Hz, 4H), 8.11 (s, 8H), 8.05 (s, 8H), 7.76 (d, J = 8 Hz, 2H), 7.74 (s, 4H), 7.60 (s, 2H), 7.58 (d, J = 8 Hz, 2H), 4.73 (s, 2H), 4.39 (s, 2H), 4.13 (s, 5H), 1.47 (s, 72H), 1.35 (s, 36H), −1.59 (brs, 2H), −2.10 pm (brs, 4H); MALDI-TOF MS (positive mode): *m/z*: 2660 [*M*+H$^+$]; FTIR (KBr): $\tilde{\nu}$=3440, 3315, 2962, 2360, 1696, 1590, 1527, 1474, 1360, 1315, 1246, 1164, 973, 916, 798, 716 cm^{-1}.

Fc-(H_2P)$_3$-C_{60}: C_{60} (11.6 mg, 0.0161 mmol), **5** (5.4 mg, 0.0020 mmol), and *N*-methylglycine (143 mg, 1.61 mmol) in dry toluene (35 mL) were refluxed overnight under nitrogen (1 atm) in the dark. The reaction mixture was allowed to cool to room temperature and then evaporated to dryness at reduced pressure. Flash column chromatography on silica gel with benzene/ethyl acetate (19:1) as eluent (R_f = 0.50) and subsequent reprecipitation from chloroform/methanol gave **Fc-(H_2P)$_3$-C_{60}** as a dark grayish-brown solid (4.5 mg, 0.0013 mmol, 65%). M.p. > 300 °C; ^{1}H NMR (270 MHz, $CDCl_2CDCl_2$, 80 °C) δ = 9.01 (d, J = 5 Hz, 2H), 8.99 (d, J = 5 Hz, 2H), 8.94 (d, J = 5 Hz, 2H), 8.89 (d, J = 5 Hz, 2H), 8.76 (d, J = 5 Hz, 2H), 8.74 (d, J = 5 Hz, 4H), 8.72 (d, J = 5 Hz, 2H), 8.51 (d, J = 8 Hz, 2H), 8.44 (brs, 1H), 8.41 (brs, 1H), 8.34 (d, J = 8 Hz, 2H), 8.31 (d, J = 5 Hz, 2H), 8.29 (d, J = 5 Hz, 2H), 8.23 (d, J = 5 Hz, 2H), 8.22 (d, J = 5 Hz, 2H), 8.15 (d, J = 2 Hz, 4H), 8.14 (d, J = 2 Hz, 4H), 8.11 (d, J = 2 Hz, 4H), 8.30–8.10 (brs, 4H), 7.96 (d, J = 8 Hz, 2H), 7.91 (d, J = 8 Hz, 2H), 7.79 (t, J = 2 Hz, 4H), 7.78 (d, J = 8 Hz, 2H), 7.66 (t, J = 2 Hz, 2H), 7.62 (d, J = 8 Hz, 2H), 5.02 (d, J = 10 Hz, 1H), 5.00 (s, 1H), 4.74 (s, 2H), 4.41 (s, 2H), 4.30 (d, J = 10 Hz, 1H), 4.16 (s, 5H), 2.91 (s, 3H), 1.41 (s, 72H), 1.30 (s, 36H), −1.42 (brs, 2H), −1.97 ppm (brs, 4H); MALDI-TOF MS: 3407 [*M*+H$^+$]; FTIR (KBr): $\tilde{\nu}$=3318, 2959, 2357, 1682, 1592, 1521, 1475, 1362, 1313, 1245, 973, 917, 800, 715, 528 cm^{-1}.

Fc-(ZnP)$_3$-C_{60}: A saturated methanol solution of $Zn(OAc)_2$ (3 mL) was added to a solution of **Fc-(H_2P)$_3$-C_{60}** (4.5 mg, 0.0013 mmol) in $CHCl_3$ (30 mL) and refluxed for 30 min. After cooling, the reaction mixture was washed twice with water, then dried over anhydrous Na_2SO_4, and the solvent was evaporated. Flash column chromatography on silica gel with benzene/ethyl acetate (19:1) as eluent (R_f = 0.50) and subsequent reprecipitation from chloroform/methanol gave **Fc-(ZnP)$_3$-C_{60}** as a dark grayish-violet solid (100% yield, 4.5 mg, 0.0013 mmol). M.p. > 300 °C; ^{1}H NMR (270 MHz, $CDCl_2CDCl_2$, 80 °C): δ = 9.10 (d, J = 5 Hz, 4H), 9.00 (d, J = 5 Hz, 4H), 8.83 (d, J = 5 Hz, 4H), 8.82 (d, J = 5 Hz, 4H), 8.50–8.00 (m, 34H), 7.96 (d, J = 8 Hz, 2H), 7.86 (d, J = 8 Hz, 2H), 7.76 (s, 4H), 7.63 (s, 2H), 5.02 (d, J = 10 Hz, 1H), 5.00 (s, 1H), 4.80–3.00 (brs, 9H), 4.32 (d, J = 10 Hz, 1H), 2.91 (s, 3H), 1.51 (s, 72H), 1.39 ppm (s, 36H); MALDI-TOF MS: 3598 [*M*+H$^+$]; FTIR (KBr): $\tilde{\nu}$=3432, 2924, 1686, 1592, 1515, 1411, 1363, 1321, 1247, 997, 928, 822, 798, 716 cm^{-1}.

Fc-(ZnP)$_3$: This compound was synthesized from **4**, 4-aminophenylferrocene, and 4-hexadecylaniline by the method described above for **5** and **Fc-(ZnP)$_3$-C_{60}**. Dark grayish-violet solid from chloroform/methanol; yield 3%; m.p. > 300 °C; ^{1}H NMR (300 MHz, $CDCl_3$): δ = 9.07 (d, J = 5 Hz, 2H), 9.06 (d, J = 5 Hz, 2H), 8.99 (d, J = 5 Hz, 2H), 8.98 (d, J = 5 Hz, 2H), 8.72 (d, J = 5 Hz, 4H), 8.46 (d, J = 8 Hz, 2H), 8.45 (d, J = 8 Hz, 2H), 8.31 (d, J = 8 Hz, 2H), 8.29 (d, J = 8 Hz, 2H), 8.16 (brs, 1H), 8.15 (d, J = 5 Hz, 4H), 8.12 (brs, 1H), 8.09 (d, J = 2 Hz, 8H), 7.75 (d, J = 8 Hz, 2H), 7.73 (d, J = 8 Hz, 2H), 7.70 (t, J = 2 Hz, 4H), 7.59 (d, J = 8 Hz, 2H), 7.29 (d, J = 8 Hz, 2H), 4.70 (t, J = 2 Hz, 2H), 4.36 (t, J = 2 Hz, 2H), 4.10 (s, 5H), 2.67 (d, J = 7 Hz, 2H), 1.60–1.20 (m, 28H), 1.44 (s, 72H), 0.89 ppm (t, J = 7 Hz, 3H); MALDI-TOF MS (positive mode): *m/z*: 3046 [*M*+H$^+$]; FTIR (KBr): $\tilde{\nu}$=3437, 2962, 2359, 1654, 1592, 1523, 1413, 1364, 1323, 1246, 997, 928, 823, 796, 715 cm^{-1}.

Compound 6: This was synthesized from **4**, 4-hexadecylaniline, and 2-(4-aminophenyl)-5,5-dimethyl-1,3-dioxane by the method described above for **5**. Dark grayish-violet solid from chloroform/methanol; yield 17%; m.p. > 300 °C; ^{1}H NMR (300 MHz, $CDCl_3$): δ = 10.03 (s, 1H), 8.96 (d, J = 5 Hz, 2H), 8.95 (d, J = 5 Hz, 2H), 8.88 (d, J = 5 Hz, 2H), 8.87 (d, J = 5 Hz, 2H), 8.63 (d, J = 5 Hz, 4H), 8.48 (d, J = 8 Hz, 2H), 8.44 (d, J = 8 Hz, 2H), 8.36 (d, J = 8 Hz, 2H), 8.32 (brs, 1H), 8.31 (d, J = 8 Hz, 2H), 8.11 (d, J = 5 Hz, 2H), 8.10 (d, J = 5H, 2H), 8.09 (brs, 1H), 8.07 (d, J = 2 Hz, 8H), 8.04 (s, 4H), 7.73 (d, J = 8 Hz, 2H), 7.71 (t, J = 2 Hz, 4H), 7.29 (d, J = 8 Hz, 2H), 2.67 (d, J = 7 Hz, 2H), 1.60–1.20 (m, 28H), 1.44 (s, 72H), 0.89 (t, J = 7 Hz, 3H), −2.15 ppm (brs, 4H); MALDI-TOF MS (positive mode): *m/z*: 2699 [*M*+H$^+$]; FTIR (KBr): $\tilde{\nu}$= 3443, 3315, 2959, 2359, 1690, 1588, 1515, 1246, 973, 911, 797, 716 cm^{-1}.

(ZnP)$_3$-C_{60}: This compound was synthesized from **6**, *N*-methylglycine, and C_{60} by the method described above for **Fc-(ZnP)$_3$-C_{60}**. Dark grayish-violet solid from chloroform/methanol; yield 49%; m.p. > 300 °C; ^{1}H NMR (300 MHz, $CDCl_2CDCl_2$, 80 °C): δ = 9.10 (d, J = 5 Hz, 2H), 9.06 (d, J = 5 Hz, 2H), 9.02 (d, J = 5 Hz, 2H), 8.88 (d, J = 5 Hz, 2H), 8.80 (d, J = 5 Hz, 2H), 8.74 (d, J = 5 Hz, 2H), 8.50 (d, J = 8 Hz, 2H), 8.31 (d, J = 8 Hz, 2H), 8.21 (d, J = 5 Hz, 2H), 8.16 (brs, 1H), 8.15 (d, J = 5 Hz, 2H), 8.13 (d, J = 2 Hz, 4H), 8.12 (brs, 1H), 8.11 (d, J = 2 Hz, 4H), 8.09 (d, J = 8 Hz, 2H), 7.93 (brs, 2H), 7.84 (d, J = 8 Hz, 2H), 7.78 (d, J = 8 Hz, 2H), 7.75 (t, J = 2 Hz, 4H), 7.73 (d, J = 8 Hz, 2H), 7.33 (d, J = 8 Hz, 2H), 4.92 (d, J = 10 Hz, 1H), 4.85 (s, 1H), 4.19 (d, J = 10 Hz, 1H), 2.85 (s, 3H), 2.71 (d, J = 7 Hz, 2H), 1.60–1.20 (m, 28H), 1.44 (s, 72H), 0.93 ppm (t, J = 7 Hz, 3H); MALDI-TOF MS (positive mode): *m/z*: 3639 [*M*+H$^+$]; FTIR (KBr): $\tilde{\nu}$=3438, 2959, 2359, 1686, 1592, 1515, 1361, 1321, 1247, 997, 929, 823, 796, 715, 527 cm^{-1}.

(ZnP)$_3$-ref: This compound was synthesized from **4** and 4-hexadecylaniline by the method described for **5** and **Fc-(ZnP)$_3$-C_{60}** above. Dark grayish-violet solid from chloroform/methanol; yield 11%; m.p. > 300 °C; ^{1}H NMR (300 MHz, $CDCl_3$): δ = 9.06 (d, J = 5 Hz, 4H), 8.98 (d, J = 5 Hz, 4H), 8.72 (d, J = 5 Hz, 4H), 8.45 (d, J = 8 Hz, 4H), 8.29 (d, J = 8 Hz, 4H), 8.14 (d, J = 5 Hz, 4H), 8.12 (brs, 2H), 8.09 (d, J = 2 Hz, 8H), 7.72 (d, J = 8 Hz, 4H), 7.70 (t, J = 2 Hz, 4H), 7.29 (d, J = 8 Hz, 4H), 2.67 (t, J = 7 Hz, 4H), 1.60–1.20 (m, 56H), 1.44 (s, 72H), 0.89 ppm (t, J = 7 Hz, 6H); MALDI-TOF MS (positive mode): *m/z*: 3086 [*M*+H$^+$]; FTIR (KBr): $\tilde{\nu}$=3432, 2924, 1686, 1592, 1519, 1409, 1360, 1319, 1246, 997, 929, 823, 796, 715 cm^{-1}.

Spectral measurements: Time-resolved fluorescence spectra were measured by a single-photon counting method using second harmonic generation (SHG, 410 nm) of a Ti:sapphire laser (Spectra-Physics, Tsunami 3950-L2S, 1.5 ps fwhm) and a streakscope (Hamamatsu Photonics,

C4334-01) equipped with a polychromator (Acton Research, SpectraPro 150) as an excitation source and detector, respectively.

Picosecond transient absorption spectra were recorded by the pump and probe method. The samples were excited with second harmonic generation (SHG, 388 nm) of output from a femtosecond Ti:sapphire regenerative amplifier seeded by SHG of an Er-doped fiber (Clark-MXRCPA-2001 plus, 1 kHz, fwhm 150 fs). The excitation light was depolarized. The monitor white light was generated by focusing the fundamental of the laser light on a flowing D_2O/H_2O cell. The transmitted monitor light was detected with a dual MOS linear image sensor (Hamamatsu Photonics, C6140) or an InGaAs photodiode array (Hamamatsu Photonics, C5890–128).

Nanosecond transient absorption measurements were carried out using SHG (530 nm) of a Nd:YAG laser (Spectra-Physics, Quanta-Ray GCR-130, fwhm 6 ns) as an excitation source. For transient absorption spectra in the near-IR region (600–1600 nm), monitoring light from a pulsed Xe lamp was detected with a Ge avalanche photodiode (Hamamatsu Photonics, B2834). Photoinduced events in nano- and microsecond time regions were estimated by using a continuous Xe lamp (150 W) and an InGaAs-PIN photodiode (Hamamatsu Photonics, G5125–10) as a probe light and detector, respectively. Details of the transient absorption measurements have been described elsewhere.[36] All the samples (10^{-4}–10^{-5} M) in a quartz cell (1 cm × 1 cm) were deaerated by bubbling argon through the solution for 15 min.

The quantum yields were measured by the comparative method.[27b] The strong monofunctionalized fullerene triplet–triplet absorption ($\varepsilon_{700\,nm}$ = 16100 $M^{-1}\,cm^{-1}$; $\Phi_{triplet}$ = 0.98)[27b] served as probe to obtain the quantum yield for the CS state, especially for the monofunctionalized fullerene π-radical anion ($\varepsilon_{1000\,nm}$ = 4700 $M^{-1}\,cm^{-1}$).[27b]

ESR measurements: The ESR spectra of the porphyrin–fullerene linked compounds and the reference compounds (1.0×10^{-5} M) in frozen DMF and PhCN were measured under photoirradiation with the focused light of a 1000 W high-pressure Hg lamp (Ushio-USH1005D) through an aqueous filter at 163 K using an attached variable-temperature apparatus in the cavity of the ESR spectrometer. The formation of $\mathbf{C_{60}}^{\bullet-}$**-ref** was examined in the ESR spectrum of $\mathbf{C_{60}}$**-ref** (1.0×10^{-4} M) in the presence of semiquinone radical anion (1.0×10^{-4} M). Tetramethylammonium hydroxide (TMAOH) was used for generation of the semiquinone radical anion in the reaction between hydroquinone and *p*-benzoquinone.[37] All ESR measurements were performed on a JEOL X-band spectrometer (JES-ME-1X) with a quartz ESR tube (3.9 mm i.d.). The *g* values and hyperfine splitting constants were calibrated using an Mn^{2+} marker.

Electrochemical measurements: The differential pulse voltammetry measurements were performed on a BAS 50 W electrochemical analyzer in a deaerated PhCN (or THF and DMF) solution containing 0.10 M *n*-Bu_4NPF_6 as a supporting electrolyte at 298 K (10 mV s^{-1}). The platinum working electrode was polished with BAS polishing alumina suspension and rinsed with acetone before use. The counter-electrode was a platinum wire. The measured potentials were recorded with respect to an Ag/$AgNO_3$ (0.01 M) reference electrode. Ferrocene/ferricenium was used as an external standard.

DFT calculations: The Gaussian 98 package[38] was used on an SGI Origin 3800 instrument. We employed the B3LYP functional and LanL2MB basis set. The vibrational frequency analysis was performed for the optimized structure to confirm it to be a stable minimum.

Acknowledgment

This work was supported by Grants-in-Aid (No. 11740352 to H.I., Nos. 11555230 and 11694079 to S.F.) and a Development of Innovative Technology (No. 12310) award from the Ministry of Education, Culture, Sports, Science and Technology, Japan. H.I. thanks the Nagase Foundation for financial support. Computation time was provided by the Supercomputer Laboratory, Institute for Chemical Research, Kyoto University.

[1] a) *Anoxygenic Photosynthetic Bacteria* (Eds.: R. E. Blankenship, M. T. Madigan, C. E. Bauer), Kluwer Academic Publishers, Dordrecht, **1995**; b) *The Photosynthetic Reaction Center* (Eds.: J. Deisenhofer, J. R. Norris), Academic Press, San Diego, **1993**.

[2] a) J. Deisenhofer, O. Epp, K. Miki, R. Huber, H. Michel, *J. Biol. Chem.* **1984**, *259*, 385; b) G. McDermott, S. M. Prince, A. A. Freer, A. M. Hawthornthwaite-Lawless, M. Z. Papiz, R. J. Cogdell, N. W. Isaacs, *Nature* **1995**, *374*, 517.

[3] a) D. Gust, T. A. Moore in *The Porphyrin Handbook, Vol. 8* (Eds.: K. M. Kadish, K. Smith, R. Guilard), Academic Press, San Diego, CA, **2000**, pp. 153–190; b) D. Gust, T. A. Moore, A. L. Moore, *Acc. Chem. Res.* **1993**, *26*, 198; c) D. Gust, T. A. Moore, A. L. Moore, *Acc. Chem. Res.* **2001**, *34*, 40.

[4] a) M. R. Wasielewski, *Chem. Rev.* **1992**, *92*, 435; b) W. B. Davis, W. A. Svec, M. A. Ratner, M. R. Wasielewski, *Nature* **1998**, *396*, 60; c) H. Kurreck, M. Huber, *Angew. Chem.* **1995**, *107*, 929; *Angew. Chem. Int. Ed. Engl.* **1995**, *34*, 849; d) M. N. Paddon-Row, *Acc. Chem. Res.* **1994**, *27*, 18; e) P. Piotrowiak, *Chem. Soc. Rev.* **1999**, *28*, 143.

[5] a) J.-C. Chambron, S. Chardon-Noblat, A. Harriman, V. Heitz, J.-P. Sauvage, *Pure Appl. Chem.* **1993**, *65*, 2343; b) A. Harriman, J.-P. Sauvage, *Chem. Soc. Rev.* **1996**, *25*, 41; c) M.-J. Blanco, M. C. Jiménez, J.-C. Chambron, V. Heitz, M. Linke, J.-P. Sauvage, *Chem. Soc. Rev.* **1999**, *28*, 293; d) V. Balzani, A. Juris, M. Venturi, S. Campagna, S. Serroni, *Chem. Rev.* **1996**, *96*, 759; e) *Electron Transfer in Chemistry* (Ed.: V. Balzani), Wiley-VCH, Weinheim, **2001**.

[6] a) H. Imahori, Y. Sakata, *Adv. Mater.* **1997**, *9*, 537; b) H. Imahori, Y. Sakata, *Eur. J. Org. Chem.* **1999**, 2445; c) S. Fukuzumi, D. M. Guldi in *Electron Transfer in Chemistry, Vol. 2* (Ed.: V. Balzani), Wiley-VCH, Weinheim, **2001**, pp. 270–337; d) H. Imahori, Y. Mori, Y. Matano, *J. Photochem. Photobiol. C* **2003**, *4*, 51.

[7] a) K. Maruyama, A. Osuka, N. Mataga, *Pure Appl. Chem.* **1994**, *66*, 867; b) A. Osuka, N. Mataga, T. Okada, *Pure Appl. Chem.* **1997**, *69*, 797; c) H. Heitele, F. Pöllinger, T. Häberle, M. E. Michel-Beyerle, H. A. Staab, *J. Phys. Chem.* **1994**, *98*, 7402; d) T. Häberle, J. Hirsch, F. Pöllinger, H. Heitele, M. E. Michel-Beyerle, C. Ander, A. Döhling, C. Krieger, A. Rückemann, H. A. Staab, *J. Phys. Chem.* **1996**, *100*, 18269; e) K. Kilsa, J. Kajanus, A. N. Macpherson, J. Martensson, B. Albinsson, *J. Am. Chem. Soc.* **2001**, *123*, 3069.

[8] a) V. S.-Y. Lin, S. G. DiMagno, M. J. Therien, *Science* **1994**, *264*, 1105; b) Y. K. Kang, I. V. Rubtsov, P. M. Iovine, J. Chen, M. J. Therien, *J. Am. Chem. Soc.* **2002**, *124*, 8275; c) H. L. Anderson, S. J. Martin, D. D. C. Bradley, *Angew. Chem. Int. Ed. Engl.* **1994**, *33*, 655; d) E. K. L. Yeow, K. P. Ghiggino, J. N. H. Reek, M. J. Crossley, A. W. Bosman, A. P. H. J. Schenning, E. W. Meijer, *J. Phys. Chem.* **2000**, *104*, 2596; e) M.-S. Choi, T. Aida, T. Yamazaki, I. Yamazaki, *Chem. Eur. J.* **2002**, *8*, 2667.

[9] a) P. J. F. de Rege, S. A. Williams, M. J. Therien, *Science* **1995**, *269*, 1409; b) H. Imahori, M. Arimura, T. Hanada, Y. Nishimura, I. Yamazaki, Y. Sakata, S. Fukuzumi, *J. Am. Chem. Soc.* **2001**, *123*, 335; c) R. W. Wagner, T. E. Johnson, J. S. Lindsey, *J. Am. Chem. Soc.* **1996**, *118*, 11166; d) J. Li, A. Ambroise, S. I. Yang, J. R. Diers, J. Seth, C. R. Wack, D. F. Bocian, D. Holten, J. S. Lindsey, *J. Am. Chem. Soc.* **1999**, *121*, 8927; e) R. K. Lammi, A. Ambroise, T. Balasubramanian, R. W. Wagner, D. F. Bocian, D. Holten, J. S. Lindsey, *J. Am. Chem. Soc.* **2000**, *122*, 7579.

[10] a) D. I. Schuster, P. Cheng, S. R. Wilson, V. Prokhorenko, M. Katterle, A. R. Holzwarth, S. E. Braslavsky, G. Klihm, R. W. Williams, C. Luo, *J. Am. Chem. Soc.* **1999**, *121*, 11599; b) N. V. Tkachenko, L. Rantala, A. Y. Tauber, J. Helaja, P. H. Hynninen, H. Lemmetyinen, *J. Am. Chem. Soc.* **1999**, *121*, 9378; c) N. V. Tkachenko, E. Vuorimaa, T. Kesti, A. S. Alekseev, A. Y. Tauber, P. H. Hynninen, H. Lemmetyinen, *J. Phys. Chem. B* **2000**, *104*, 6371; d) F. D'Souza, G. R. Deviprasad, M. E. El-Khouly, M. Fujitsuka, O. Ito, *J. Am. Chem. Soc.* **2001**, *123*, 5277.

[11] a) J. W. Verhoeven, *Adv. Chem. Phys.* **1999**, *196*, 603; b) L. Sun, L. Hammarström, B. Åkermark, S. Styring, *Chem. Soc. Rev.* **2001**, *30*, 36; c) N. Armaroli, *Chem. Soc. Rev.* **2001**, *30*, 113; d) N. Armaroli, *Photochem. Photobiol. Sci.* **2003**, *2*, 73; e) J.-F. Nierengarten, N. Armaroli, G. Accorsi, Y. Rio, J.-F. Eckert, *Angew. Chem. Int. Ed.* **2003**, *42*, 37; f) J.-F. Eckert, J. F. Nicoud, J.-F. Nierengarten, S.-G. Liu, L.

Echegoyen, F. Barigelletti, N. Armaroli, L. Ouali, V. Krasnikov, G. Hadziioannou, *J. Am. Chem. Soc.* **2000**, *122*, 7467.

[12] a) D. Kuciauskas, P. A. Liddell, S. Lin, T. E. Johnson, S. J. Weghorn, J. S. Lindsey, A. L. Moore, T. A. Moore, D. Gust, *J. Am. Chem. Soc.* **1999**, *121*, 8604; b) A. Nakano, T. Yamazaki, Y. Nishimura, I. Yamazaki, A. Osuka, *Chem. Eur. J.* **2000**, *6*, 3254; c) H. Imahori, H. Norieda, H. Yamada, Y. Nishimura, I. Yamazaki, Y. Sakata, S. Fukuzumi, *J. Am. Chem. Soc.* **2001**, *123*, 100.

[13] H. Imahori, D. M. Guldi, Y. Yoshida, C. Luo, Y. Sakata, S. Fukuzumi, *J. Am. Chem. Soc.* **2001**, *123*, 6617.

[14] a) A. Osuka, H. Shimidzu, *Angew. Chem. Int. Ed. Engl.* **1997**, *36*, 135; b) N. Aratani, A. Osuka, Y. H. Kim, D. H. Jeong, D. Kim, *Angew. Chem. Int. Ed.* **2000**, *39*, 1458; c) N. Aratani, A. Osuka, H. S. Cho, D. Kim, *J. Photochem. Photobiol. C* **2002**, *3*, 25.

[15] a) N. Ohta, Y. Iwaki, T. Ito, I. Yamazaki, A. Osuka, *J. Phys. Chem. B* **1999**, *103*, 11242; b) J. J. Piet, P. N. Taylor, H. L. Anderson, A. Osuka, J. M. Warman, *J. Am. Chem. Soc.* **2000**, *122*, 1749; c) Y. H. Kim, D. H. Jeong, D. Kim, S. C. Jeoung, H. S. Cho, S. K. Kim, N. Aratani, A. Osuka, *J. Am. Chem. Soc.* **2001**, *123*, 76.

[16] a) K. Susumu, T. Shimidzu, K. Tanaka, H. Segawa, *Tetrahedron Lett.* **1996**, *37*, 8399; b) R. G. Khoury, L. Jaquinod, K. M. Smith, *Chem. Commun.* **1997**, 1057; c) M. G. H. Vicente, L. Jaquinod, K. M. Smith, *Chem. Commun.* **1999**, 1771; d) M. A. Miller, R. K. Lammi, S. Prathapan, D. Holten, J. S. Lindsey, *J. Org. Chem.* **2000**, *65*, 6634; e) C. Clausen, D. T. Gryko, A. A. Yasseri, J. R. Diers, D. F. Bocian, W. G. Kuhr, J. S. Lindsey, *J. Org. Chem.* **2000**, *65*, 7371.

[17] D. Bonifazi, F. Diederich, *Chem. Commun.* **2002**, 2178.

[18] H. Imahori, K. Tamaki, Y. Araki, Y. Sekiguchi, O. Ito, Y. Sakata, S. Fukuzumi, *J. Am. Chem. Soc.* **2002**, *124*, 5165.

[19] H. Imahori, K. Tamaki, D. M. Guldi, C. Luo, M. Fujitsuka, O. Ito, Y. Sakata, S. Fukuzumi, *J. Am. Chem. Soc.* **2001**, *123*, 2607.

[20] Q. M. Wang, D. W. Bruce, *Synlett* **1995**, 1267.

[21] M. S. Newman, L. F. Lee, *J. Org. Chem.* **1972**, *37*, 4468.

[22] H. Imahori, T. Azuma, A. Ajavakom, H. Norieda, H. Yamada, Y. Sakata, *J. Phys. Chem. B* **1999**, *103*, 7233.

[23] M. Maggini, G. Scorrano, M. Prato, *J. Am. Chem. Soc.* **1993**, *115*, 9798.

[24] a) H. Imahori, K. Hagiwara, M. Aoki, T. Akiyama, S. Taniguchi, T. Okada, M. Shirakawa, Y. Sakata, *J. Am. Chem. Soc.* **1996**, *118*, 11771; b) H. Imahori, M. E. El-Khouly, M. Fujitsuka, O. Ito, Y. Sakata, S. Fukuzumi, *J. Phys. Chem. A* **2001**, *105*, 325.

[25] Exciton delocalization in singlet and triplet excited states was reported in similar *meso*,*meso*-linked zinc porphyrin arrays. See ref. [15b,c].

[26] S. Fukuzumi, K. Miyamoto, T. Suenobu, E. Van Caemelbecke, K. M. Kadish, *J. Am. Chem. Soc.* **1998**, *120*, 2880.

[27] a) D. M. Guldi, H. Hungerbühler, K.-D. Asmus, *J. Phys. Chem.* **1995**, *99*, 9380; b) C. Luo, D. M. Guldi, H. Imahori, K. Tamaki, Y. Sakata, *J. Am. Chem. Soc.* **2000**, *122*, 6535.

[28] a) S. Fukuzumi, S. Mochizuki, T. Tanaka, *Inorg. Chem.* **1989**, *28*, 2459; b) S. Fukuzumi, K. Okamoto, Y. Yoshida, H. Imahori, Y. Araki, O. Ito, *J. Am. Chem. Soc.* **2003**, *125*, 1007.

[29] Taking into account the additional pathway, namely, **Fc-^{1}(ZnP)$_2^*$-C$_{60}$**$\rightarrow$**Fc-^{3}(ZnP)$_2^*$-C$_{60}$**$\rightarrow$**Fc-(ZnP)$_2^{\cdot+}$-C$_{60}^{\cdot-}$**$\rightarrow$**Fc$^+$-(ZnP)$_2$-C$_{60}^{\cdot-}$** in the **Fc-(ZnP)$_2$-C$_{60}$** tetrad, the total quantum yields for the formation of the final charge-separated state in **Fc-(ZnP)$_2$-C$_{60}$** are corrected to 0.88 (PhCN), 0.82 (THF), and 0.92 (DMF), respectively.

[30] S. Fukuzumi, H. Mori, T. Suenobu, H. Imahori, X. Gao, K. M. Kadish, *J. Phys. Chem. A* **2000**, *104*, 10688.

[31] (**Fc-ref**)$^+$ produced by the oxidation with $[Ru(bpy)_3]^{3+}$ exhibits no detectable ESR signal because of the fast relaxation time under the same experimental conditions.

[32] The spin distribution of the porphyrin trimer radical cation could not be determined experimentally because of broadening of the ESR signal of the radical cation. Localization of the porphyrin cation radical is reported in a similar *meso*,*meso*-linked porphyrin dimer system. See: H. Segawa, D. Machida, Y. Senshu, J. Nakazaki, K. Hirakawa, F. Wu, *Chem. Commun.* **2002**, 3032.

[33] a) D. Gust, T. A. Moore, A. L. Moore, S.-J. Lee, E. Bittersmann, D. K. Luttrull, A. A. Rehms, J. M. DeGraziano, X. C. Ma, F. Gao, R. E. Belford, T. T. Trier, *Science* **1990**, *248*, 199; b) D. Gust, T. A. Moore, A. L. Moore, A. N. Macpherson, A. Lopez, J. M. DeGraziano, I. Gouni, E. Bittersmann, G. R. Seely, F. Gao, R. A. Nieman, X. C. Ma, L. J. Demanche, S.-C. Hung, D. K. Luttrull, S.-J. Lee, P. K. Kerrigan, *J. Am. Chem. Soc.* **1993**, *115*, 11141.

[34] a) M. R. Wasielewski, G. L. Gains III, G. P. Wiederrecht, W. A. Svec, M. P. Niemczyk, *J. Am. Chem. Soc.* **1993**, *115*, 10442; b) M. R. Wasielewski, G. P. Wiederrecht, W. A. Svec, M. P. Niemczyk, *Sol. Energy Mater. Solar Cells* **1995**, *38*, 127.

[35] a) S. Fukuzumi, K. Ohkubo, H. Imahori, J. Shao, Z. Ou, G. Zheng, Y. Chen, R. K. Pandey, M. Fujitsuka, O. Ito, K. M. Kadish, *J. Am. Chem. Soc.* **2001**, *123*, 10676; b) Y.-Z. Hu, S. Tsukiji, S. Shinkai, S. Oishi, I. Hamachi, *J. Am. Chem. Soc.* **2000**, *122*, 241.

[36] M. Fujitsuka, A. Watanabe, O. Ito, K. Yamamoto, H. Funasaka, *J. Phys. Chem. A* **1997**, *101*, 7960.

[37] S. Fukuzumi, I. Nakanishi, T. Suenobu, K. M. Kadish, *J. Am. Chem. Soc.* **1999**, *121*, 3468.

[38] Gaussian 98 (Revision A.7), M. J. Frisch, G. W. Trucks, H. B. Schlegel, G. E. Scuseria, M. A. Robb, J. R. Cheeseman, V. G. Zakrzewski, J. A. Montgomery, Jr., R. E. Stratmann, J. C. Burant, S. Dapprich, J. M. Millam, A. D. Daniels, K. N. Kudin, M. C. Strain, O. Farkas, J. Tomasi, V. Barone, M. Cossi, R. Cammi, B. Mennucci, C. Pomelli, C. Adamo, S. Clifford, J. Ochterski, G. A. Petersson, P. Y. Ayala, Q. Cui, K. Morokuma, D. K. Malick, A. D. Rabuck, K. Raghavachari, J. B. Foresman, J. Cioslowski, J. V. Ortiz, B. B. Stefanov, G. Liu, A. Liashenko, P. Piskorz, I. Komaromi, R. Gomperts, R. L. Martin, D. J. Fox, T. Keith, M. A. Al-Laham, C. Y. Peng, A. Nanayakkara, C. Gonzalez, M. Challacombe, P. M. W. Gill, B. G. Johnson, W. Chen, M. W. Wong, J. L. Andres, M. Head-Gordon, E. S. Replogle, J. A. Pople, Gaussian, Inc., Pittsburgh, PA, **1998**.

Received: July 7, 2003
Revised: January 1, 2004

Published online: May 6, 2004